Transactions of the Royal Society of Edinburgh: Earth Sciences, **96,** 21–41, 2005

Protaspid ontogeny of *Bolaspidella housensis* (Order Ptychopariida, Class Trilobita), and other similar Cambrian protaspides

Dong-Chan Lee and Brian D. E. Chatterton

ABSTRACT: The protaspid ontogeny of *Bolaspidella housensis* (Walcott, 1886) is re-described. This species is known from the Marjum Formation (Lower Marjuman Stage) of western Utah, USA. Three protaspid stages are recognised, with the instars discriminated most readily by different spacing between the postero-lateral ends of the fixigena. Protaspides of *B. housensis* are shown to be similar to those of *Glaphyraspis parva*, from several Upper Cambrian localities in the USA, and Ptychopariide sp. E from the Upper Cambrian of the Wasatch Mountains in Utah, USA.

KEY WORDS: Protaspides, Marjum Formation.

Robison (1964) described protaspides of *Bolaspidella housensis* (Walcott, 1886), and figured two silicified specimens (pl. 89, figs 6, 7). Abundant silicified specimens of *B. housensis* were obtained by the present authors from limestone samples of a single sampling horizon of the Marjum Formation, House Range, western Utah, USA (Fig. 1). These specimens provide an opportunity to re-describe and re-illustrate the ontogeny of *B. housensis* in greater detail, using Scanning Electron Microscopy (SEM) techniques. Lee (2002) recently re-examined many Cambrian protaspides described by Hu during the 1960s to 1980s; see Lee (2002) and Chatterton & Speyer (*in* Whittington *et al*. 1997) for list of Hu's publications. Some protaspides that share similarities with those of *Bolaspidella housensis* are re-described and illustrated herein.

Specimens obtained by the present authors from the Marjum Formation are housed in the University of Alberta Paleontology Collection (UA); and the protaspides from other localities are housed in the Cincinnati Museum Center Paleontology Collection (CMC-P).

1. Association of protaspides from the Marjum Formation

Most of the silicified protaspides obtained from limestones of the Marjum Formation (Fig. 1) are assigned to *Bolaspidella housensis*. Few species other than *B. housensis* can be identified from the post-protaspid materials obtained; a few fragmentary cranidia and pygidia are assigned to *Modocia*. The abundance of specimens of *B. housensis*, in comparison to those of other species, indicates that the assignment of the protaspides to this species is correct.

Gradual allometric transformations support the present assignment of protaspides to *Bolaspidella housensis*. Morphological transformations are very gradual within the protaspid period; and morphological differences between specimens of the last protaspid stage and those of the early meraspid stages (Figs 2 and 3a–c) are also minor. Morphological changes are also gradual through the meraspid period and into the early holaspid period, finally transforming gradually into holaspides of *B. housensis*. No radical metamorphosis occurs in the ontogeny of *B. housensis*.

The protaspid period of *Bolaspidella housensis* is divided into three stages (instars), based on several criteria (see Fig. 2). The scatter plot diagram of length versus width of protaspides (Fig. 4a) indicates the existence of three stages. The most useful criterion for discriminating the three instars of the protaspid period of *B. housensis* is the distance between the postero-lateral corners of the fixigenae. These instars are difficult to identify purely on the basis of length/width plots of whole specimens (Figs 4, 5). The columnar chart of distances between the postero-lateral corners of the fixigenae shows small, but abrupt and significant, changes between adjacent protaspid stages. Where exoskeletal length and width are plotted against the spacing between the postero-lateral ends of the fixigenal areas (Fig. 5b, c), the instars are more distinct than in plots of length against width (Fig. 4a). The outline of the posterior margin of the exoskeleton, in posterior view, changes from semi-circular in protaspid stage 1, to transversely elongated pentagonal in stage 2, and finally to transversely elongated sub-rectangular in stage 3 (Fig. 2c, g, k).

The linear ontogenetic trajectories of plots of exoskeletal length versus width are calculated for each protaspid stage (Fig. 4b). These trajectories indicate that length increases more than width as the larvae grew. Since length is measured from the sagittal point of the indented posterior margin, however, the proportionately greater increase in length may be due in part to the fact that indentation of the posterior margin becomes progressively shallower (compare Fig. 2a, e, and i). The trajectory slope for the whole protaspid period is a factor of 1·00 (slope of 45°).

Besides the protaspides of *Bolaspidella housensis*, five different protaspid morphotypes were obtained from the same samples of the Marjum Formation (Fig. 3d–m). Due to a paucity of holaspid materials with which these protaspides can be associated, they are left in open nomenclature. A morphotype represented by the smallest specimens (Fig. 3d–g) invites detailed discussion. These specimens are smaller than, and occur in similar abundance to, those of protaspid stage 1 of *B. housensis*, suggesting that they could represent an earliest calcified protaspid stage of *B. housensis*. The morphotype differs from the protaspid stage 1 of *B. housensis* (Fig. 2a–d) in having a pair of distinct anterior pits, a relatively well-defined inverted sub-triangular frontal axial lobe, much shorter

https://doi.org/10.1017/S026359330000122X Published online by Cambridge University Press

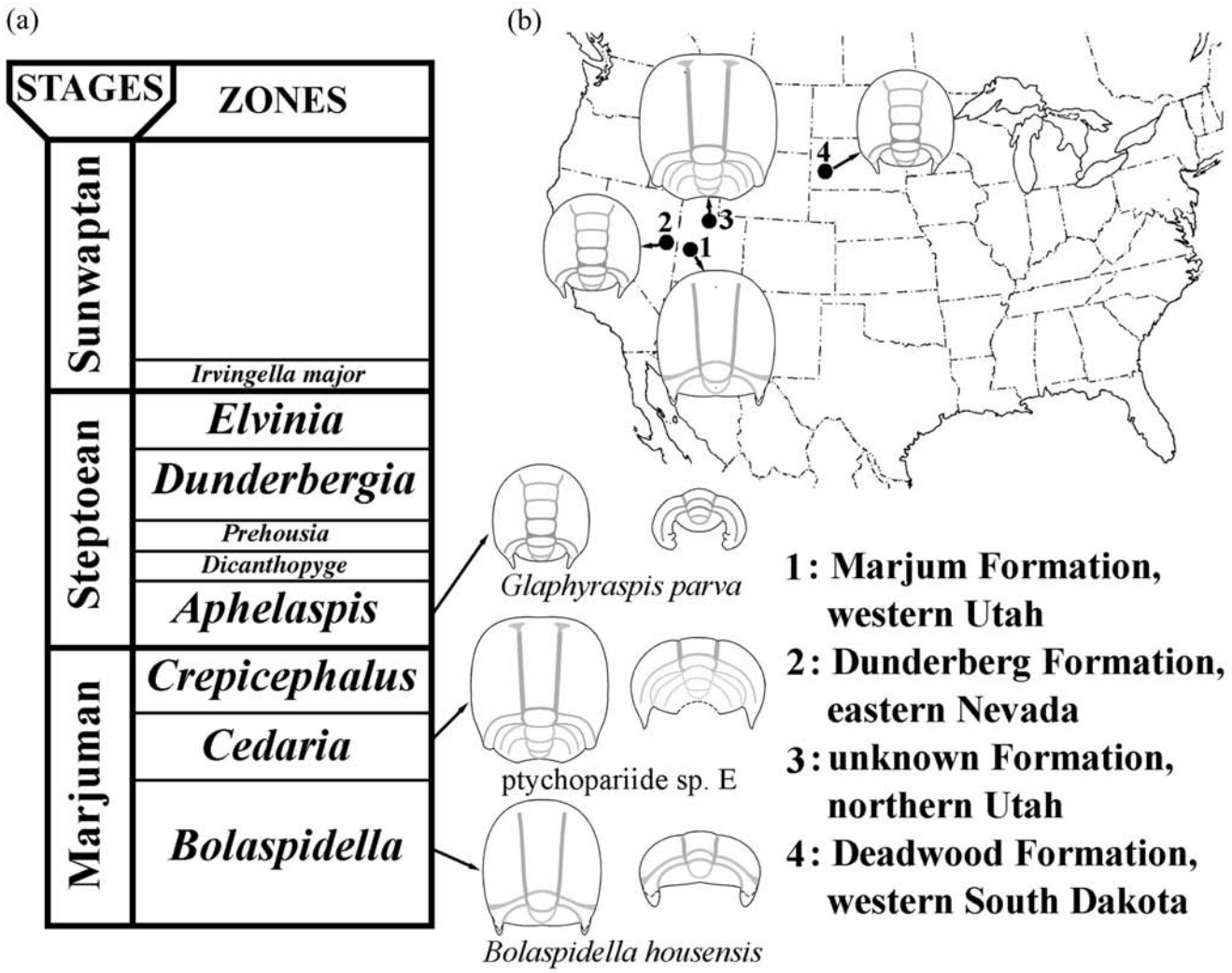

Figure 1 Geographical and stratigraphical occurrences of species described in the text: (a) Biostratigraphical; (b) Geographical: GPS reading of the sampling horizon in the Marjum Formation (1) is 39°21′25.5″ and 113°16′59.2″; GPS reading of the sampling horizon in the Dunderberg Formation (2) is 39°26′13.7″ and 114°44′34.3″.

librigenae that reach only mid-exoskeletal length, posterior fixigenal spines that are longer and more narrowly spaced, and a more flattened lateral profile. These differences may be developmental. In particular, such major changes might accompany a metamorphosis associated with a life mode change from planktonic to benthic. However, when a planktonic protaspis metamorphoses into a benthic protaspis, the lateral profile usually changes from relatively high and inflated to low and flat. The lateral profile change observed here does not agree with this generalisation. Also, other features of planktonic protaspides such as a hypostome, with long marginal spines, that is large enough in size to cover most of the ventral surface of the protaspis, do not occur in this small larva.

The plots of exoskeletal length versus width for this smallest morphotype lie below those of the protaspid stage 1 of *Bolaspidella housensis* (Fig. 6a) in such a manner that the widths are similar but the lengths are shorter. If this protaspis belongs to *B. housensis*, the scatter diagram would require that the protaspid individuals only increased their length between the first two larval stages. Some species (for example, *Calymene* n. sp. B, Chatterton *et al.* 1990, fig. 7.3) show a similar growth trend across the protaspid stages, whereas protaspides of other species (for example, *Flexicalymene senaria*, Chatterton *et al.* 1990, fig. 3.3) retain the same length versus width ratio before and after they undergo a metamorphosis. The linear trajectory slope for this small protaspis is a factor of 0·59, distinctly steeper than that of protaspid stage 1 of *B. housensis* (0·46). This steeper slope contrasts with a trend of such slopes within instars becoming progressively steeper through the protaspid ontogeny of *B. housensis* (Fig. 4a). The indentation of the posterior margin of these smallest specimens is deeper than that of protaspid stage 1. If measurements of length are made by projecting the lateral exoskeletal outline into the posterior margin, the slope is even steeper than the factor of 0·59. These observations do not allow us to assign this smallest protaspis to *B. housensis*; they are assigned to 'Ptychopariide sp. A'.

A morphotype with three pairs of fixigenal spines is among the other four protaspid morphotypes not assigned to *B. housensis* (Fig. 3h, i). The morphotype is also characterised by having a pair of distinct anterior pits, an inverted subtriangular anterior-most axial lobe, and librigenae that reach only mid-shield length. These features suggest that these larger specimens represent a later ontogenetic stage of Ptychopariide sp. A. If this were to be the case, the addition of anterior and mid-fixigenal spines can be explained as a result of a metamorphosis that also entails a large size increase. The discovery of a protaspis, 'Ptychopariide sp. B', with three pairs of fixigenal spines, similar in size to Ptychopariide sp. A (Figs 6b, 12q, r) opposes this assignment.

The other three protaspides (Fig. 3j–m), 'Ptychopariide sp. C', 'Ptychopariide sp. D', and 'Corynexochide sp. A' are rare.

https://doi.org/10.1017/S026359330000122X Published online by Cambridge University Press

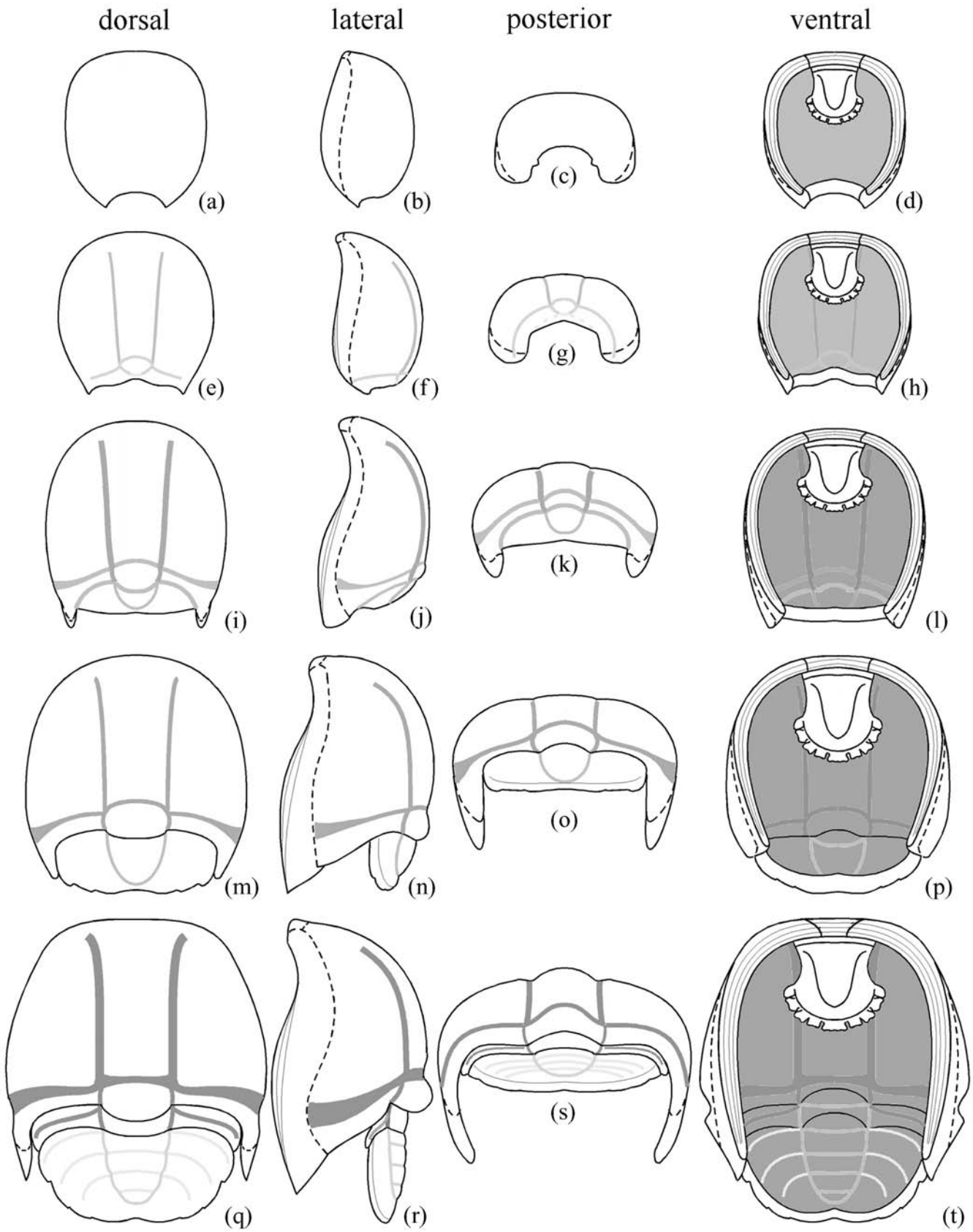

Figure 2 Reconstruction of protaspides and meraspides of *Bolaspidella housensis* (Walcott, 1886). All drawings are × 75: (a–d) protaspid stage 1; (e–h) protaspid stage 2; dotted line on posterior reconstruction (g) represents posterior cranidial marginal furrow observed in some specimens; (i–l) protaspid stage 3; (m–p) meraspid degree 0; (q–t) meraspid degree 1: the orientation of protopygidium is projected from that of meraspid degree 0 (m–p).

Ptychopariide sp. C (Fig. 3l, m) differs from *B. housensis* in having a backward-tapering exoskeleton, a well-defined anteriormost axial lobe, and blunt hypostomal border spines separated by very narrow slots. Ptychopariide sp. D protaspides (Fig. 3j) differ from *B. housensis* in lacking a ventrally extended posterior fixigenal area. Corynexochide sp. A (Fig. 3k) differs in having a nearly hexagonal exoskeleton and a sagittal furrow behind the anteriormost axial lobe. The

https://doi.org/10.1017/S026359330000122X Published online by Cambridge University Press

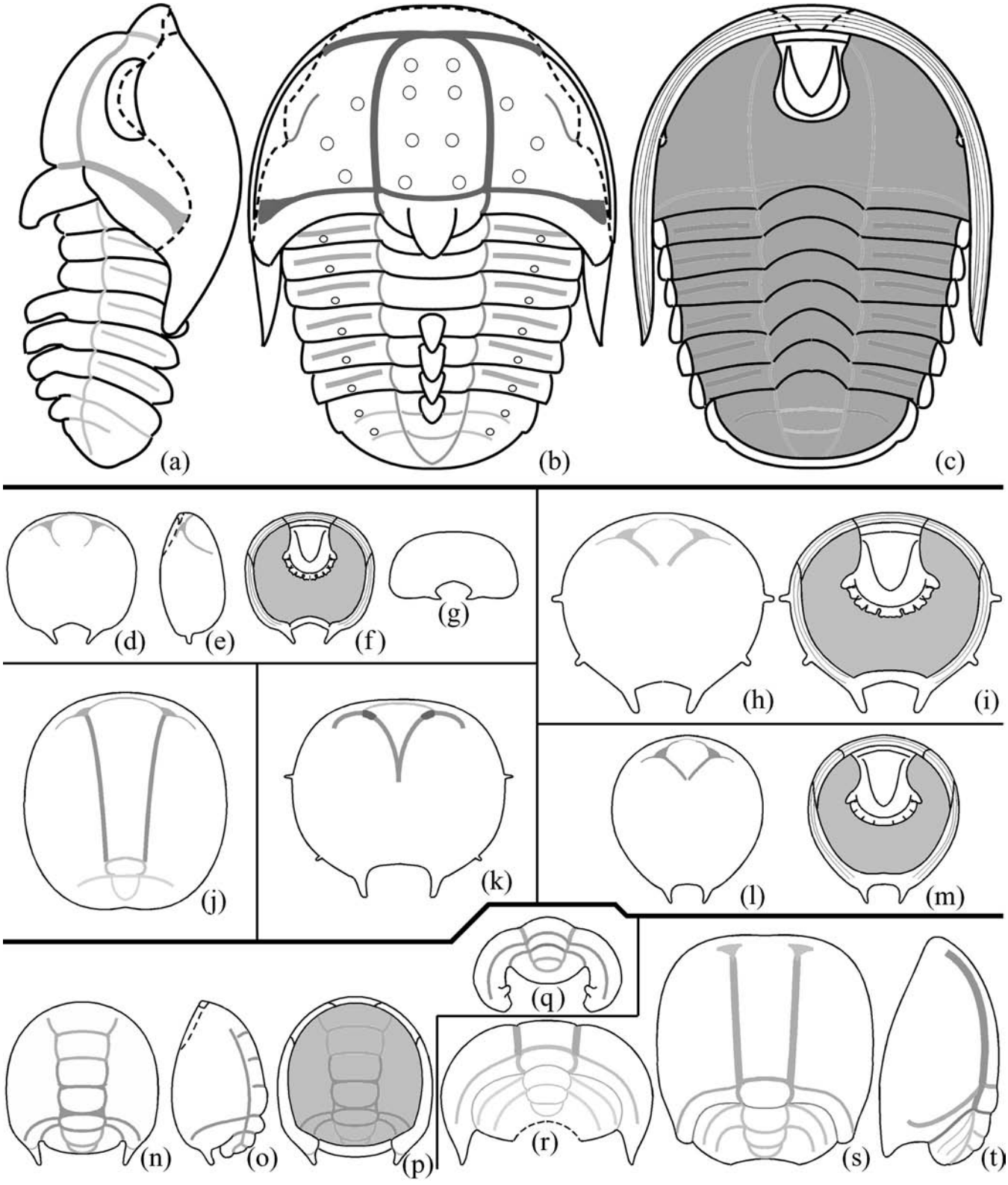

Figure 3 Reconstruction of meraspis of *Bolaspidella housensis* (Walcott, 1886), protaspides co-occurring with *B. housensis*, and protaspides similar to those of *B. housensis*. All drawings are × 75, unless otherwise noted. (a–c) Meraspid degree 6 of *Bolaspidella housensis* (Walcott, 1886), × 30: (a) lateral view; (b) dorsal view; (c) ventral view; size and shape of rostral plate is estimated upon the basis of the distance between anterior proximal ends of free cheeks (see Fig. 10m). (d–g) Protaspis of Ptychopariide sp. A: (d) dorsal view; (e) lateral view; (f) ventral view; (g) posterior view. (h, i) Protaspis of Ptychopariide sp. B: (h) dorsal view; (i) ventral view. (j) Protaspis of Ptychopariide sp. D, dorsal view. (k) Protaspis of Corynexochide sp. A, dorsal view. (l, m) Protaspis of Ptychopariide sp. C: (l) dorsal view; (m) ventral view. (n–q) Protaspid stage 2 of *Glaphyraspis parva* (Walcott, 1899): (n) dorsal view; (o) lateral view; (p) ventral view; (q) posterior view. (r–t) Protaspid stage 2 of Ptychopariide sp. E: (r) posterior view; (s) dorsal view; (t) lateral view.

https://doi.org/10.1017/S026359330000122X Published online by Cambridge University Press

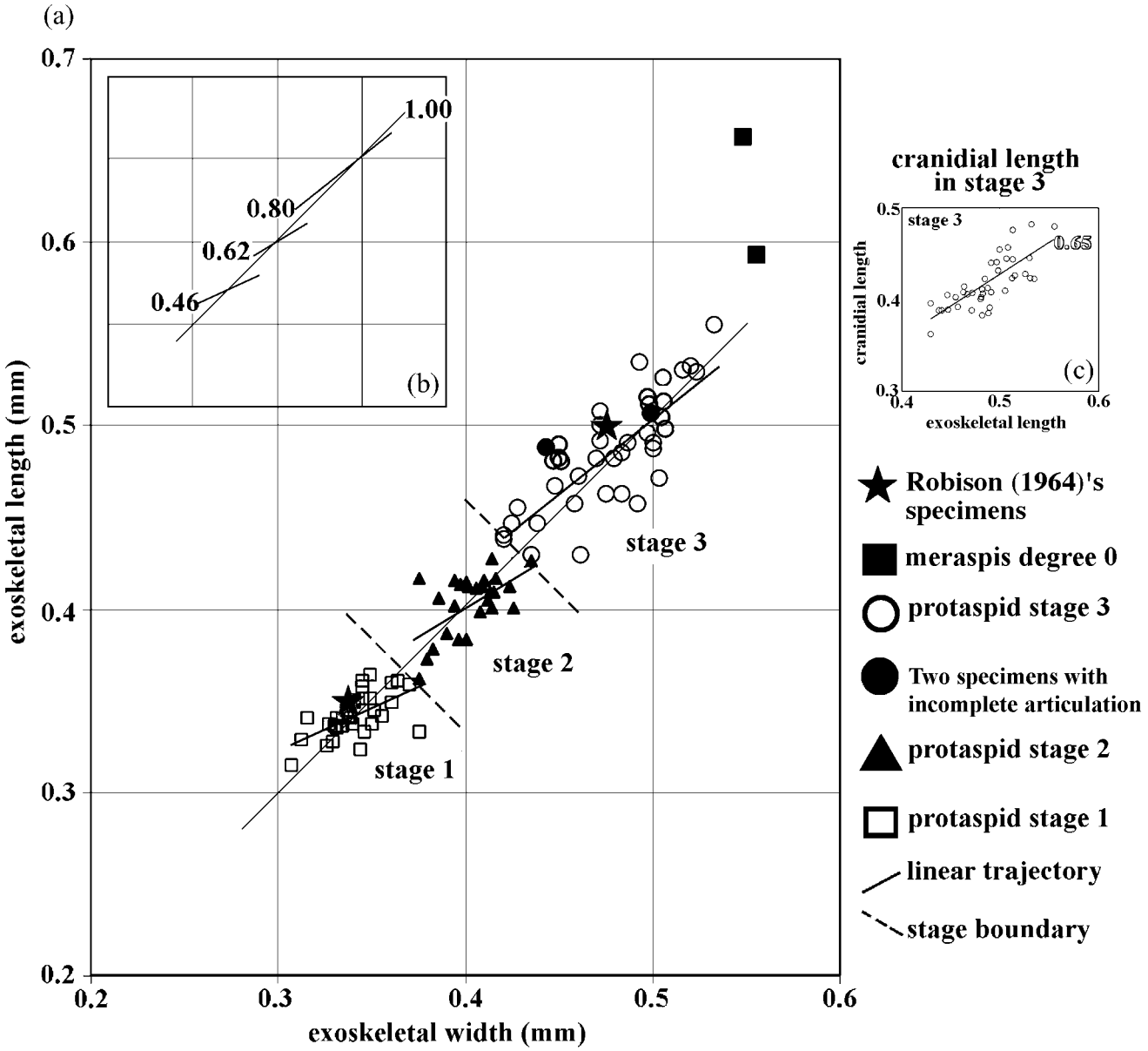

Figure 4 Scatter plot diagrams and ontogenetic linear trajectories of protaspides of *Bolaspidella housensis* (Walcott, 1886): (a) Scatter plot diagram of length versus width of protaspides and meraspid degree 0; (b) Linear ontogenetic trajectory and slope gradient representing ratio of length to width for each protaspid stage; the factor of 1·00 is calculated for the whole protaspid period; (c) Scatter plot diagram and slope gradient of cranidial length to exoskeletal length of protaspid stage 3.

plots of width versus length of all these morphotypes fall outside those of the protaspid stages assigned to *B. housensis* (Fig. 6a, b).

2. Description of protaspides from the Marjum Formation

Order Ptychopariida Swinnerton, 1915
Family Menomoniidae Walcott, 1916

Remarks. Pratt (1992, p. 77) provided the most recent account for the concept of the family.

Genus *Bolaspidella* Resser, 1937

Type species. *Ptychoparia housensis* Walcott, 1886, Wheeler Formation, Utah.

Remarks. The concept of *Bolaspidella* by Robison (1964) and Pratt (1992) is followed here.

Bolaspidella housensis (Walcott, 1886)
(Figs 2, 3a–c, 7–11)

1886 *Ptychoparia housensis* Walcott, p. 201, pl. 25, fig. 5.
1937 *Bolaspidella housensis*, Resser, p. 4.
1954 *Bolaspidella housensis*, Palmer, p. 57, pl. 16, fig. 3.
1964 *Bolaspidella housensis*, Robison, p. 555, pl. 88, figs 16–21, pl. 89, figs 1–11.

Holotype. An incomplete cranidium from 'blue-grey calcareous shale,' Antelope Springs, House Range, Utah (Walcott 1886, pl. 25, fig. 5).

Diagnosis. See Robison (1964, p. 555) for holaspid diagnosis.

Stratigraphical and geographical distributions. This species occurs in the *Bathyuriscus fimbriatus* subzone of the

https://doi.org/10.1017/S026359330000122X Published online by Cambridge University Press

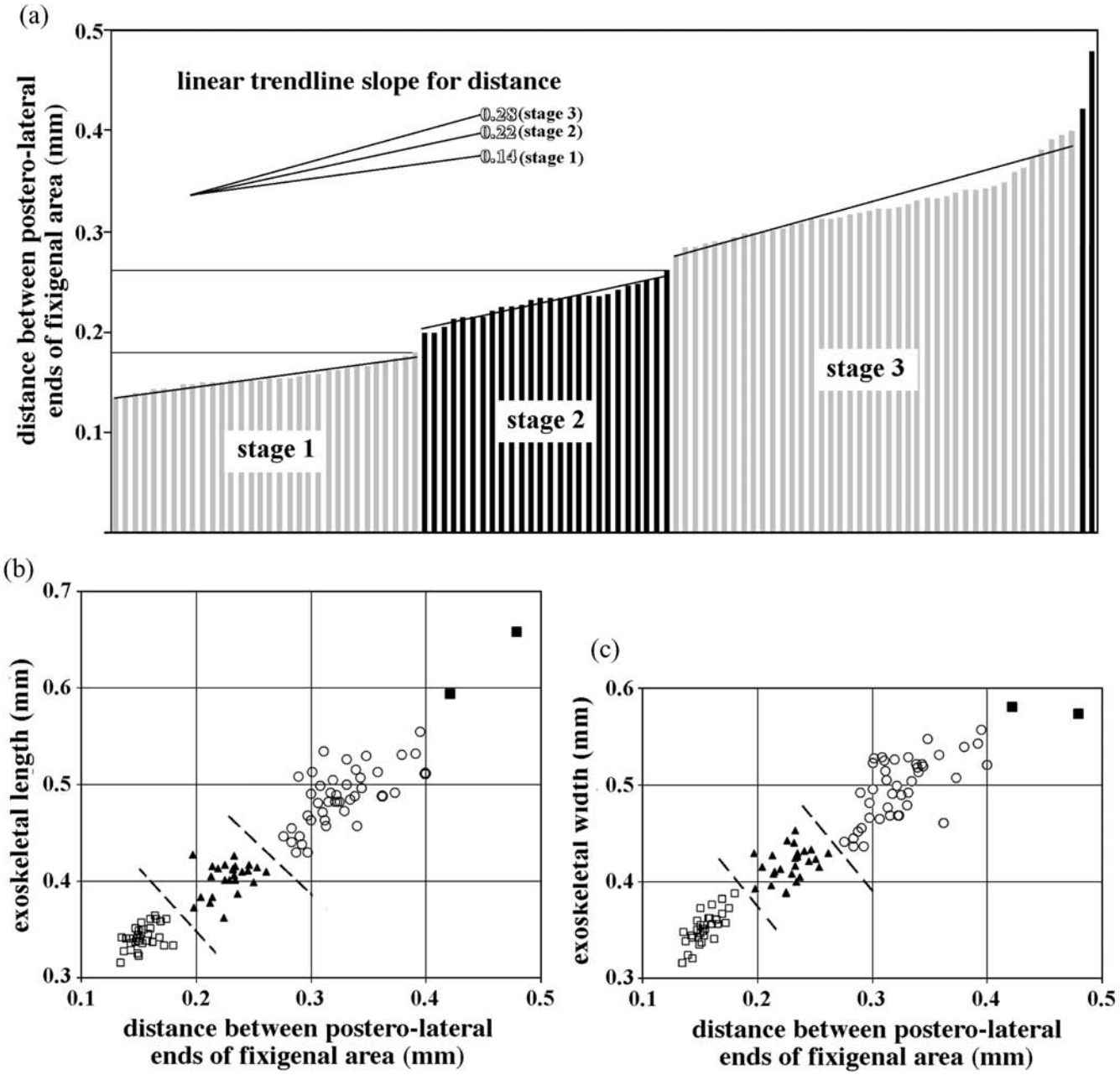

Figure 5 Columnar and scatter plot diagrams of spacing between postero-lateral ends of fixigenal area for protaspides of *Bolaspidella housensis* (Walcott, 1886): (a) Columnar diagram of distance between postero-lateral ends of fixigenal area, and slope gradient of linear trendline of measurements for each protaspid stage; (b) Scatter plot diagram of distance between postero-lateral ends of fixigenal area versus exoskeletal length. See Figure 4 for legend; (c) Scatter plot diagram of distance between postero-lateral ends of fixigenal area versus exoskeletal width. See Figure 4 for legend.

Bolaspidella Zone (Lower Marjuman Stage). It has been reported from the Wheeler and Marjum formations in western Utah, U.S.A.

Terminology. Robison (1964) recognised two protaspid stages of *Bolaspidella housensis*, anaprotaspid and metaprotaspid stages. The division follows Beecher's original definition (1895) where the differentiation of a protopygidium (formation of furrow at back of cranidium) separates the two stages. In the present work, the protaspid period of *B. housensis* is divided into three stages that are designated protaspid stages 1, 2, and 3. Anaprotaspides and metaprotaspides are not referred to because there is variation in the timing of differentiation of the protopygidium. The protopygidium is not differentiated in protaspid stage 1, and it is almost always differentiated in stage 3. However, it is differentiated to varying degrees in stage 2 (see below).

The protopygidium is identified by the development of recognisable somites behind the cephalon, and usually by the impression of a marginal furrow behind the cranidium. The first event occurs before the second in some trilobites and the two occur simultaneously in others (Chatterton & Speyer *in* Whittington *et al*. 1997). The differentiation of a protopygidium sometimes occurs in association with a life mode change (*Flexicalymene*, Chatterton *et al*. 1990). In some trilobites, the posterior cranidial marginal furrow is first impressed only in the axial region, and it extends into pleural regions in subsequent stages (*Flexicalymene*, Chatterton & Speyer, *in* Whittington *et al*. 1997, fig. 237.3) or the furrow in the lateral region remains very weakly impressed for the whole protaspid period (*Dimeropyge*, Chatterton & Speyer, *in* Whittington *et al*. 1997, fig. 160).

Some specimens of protaspid stage 2 of *Bolaspidella housensis* have a weakly impressed transverse furrow in the posterior

https://doi.org/10.1017/S026359330000122X Published online by Cambridge University Press

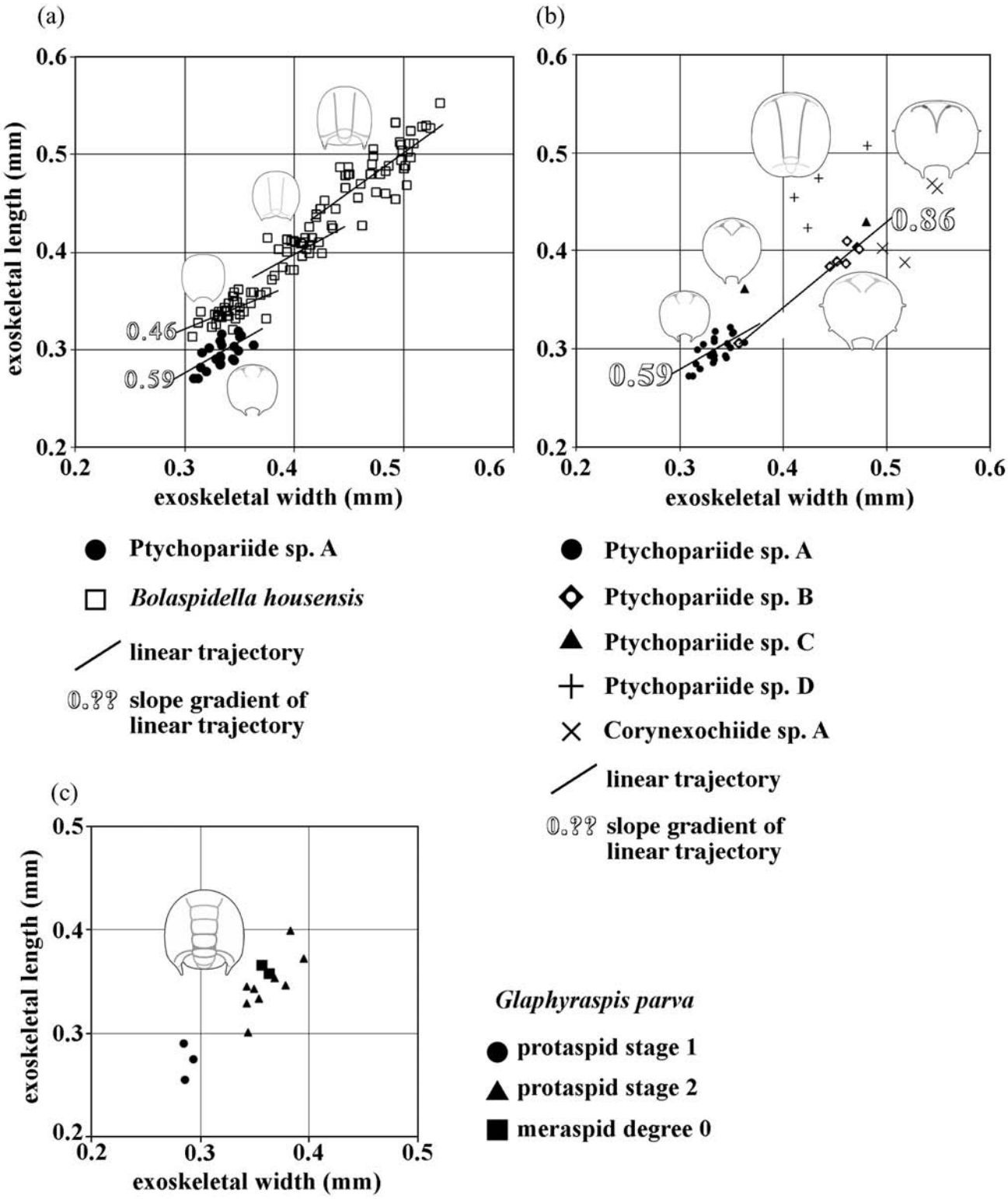

Figure 6 Scatter plot diagrams of length versus width of other protaspides: (a) Scatter plot diagram of protaspides of *Bolaspidella housensis* (Walcott, 1886) and Ptychopariide sp. A; (b) Scatter plot diagram of other protaspid morphotypes from the Marjum Formation; (c) Scatter plot diagram of *Glaphyraspis parva* (Walcott, 1889) from the Dunderberg Formation.

exoskeletal region (Fig. 7y, w). The homology of this furrow dictates whether or not the protopygidium is differentiated. In stage 3 (Fig. 8e), two furrows are impressed in the posterior part of the pleural region; the anterior is the posterior cranidial border furrow and the posterior is the posterior cranidial marginal furrow. In stage 3, the posterior cranidial border furrows reach the lateral margin, and the posterior cranidial marginal furrows meet the lateral corner of a transversely elongated, rectangular posterior margin; the corners delimit the lateral ends of the protopygidium. The posterior margin outline of stage 2 is a transversely elongated pentagon and its two lateral corners topologically correspond to those of stage 3. The single transverse furrow observed in some stage 2 specimens reaches the lateral exoskeletal margin and does not meet the lateral corners of the posterior margin. This indicates that the furrow represents the posterior cranidial border furrow. The transversely elongated narrow region behind the furrow contains future posterior cranidial border

https://doi.org/10.1017/S026359330000122X Published online by Cambridge University Press

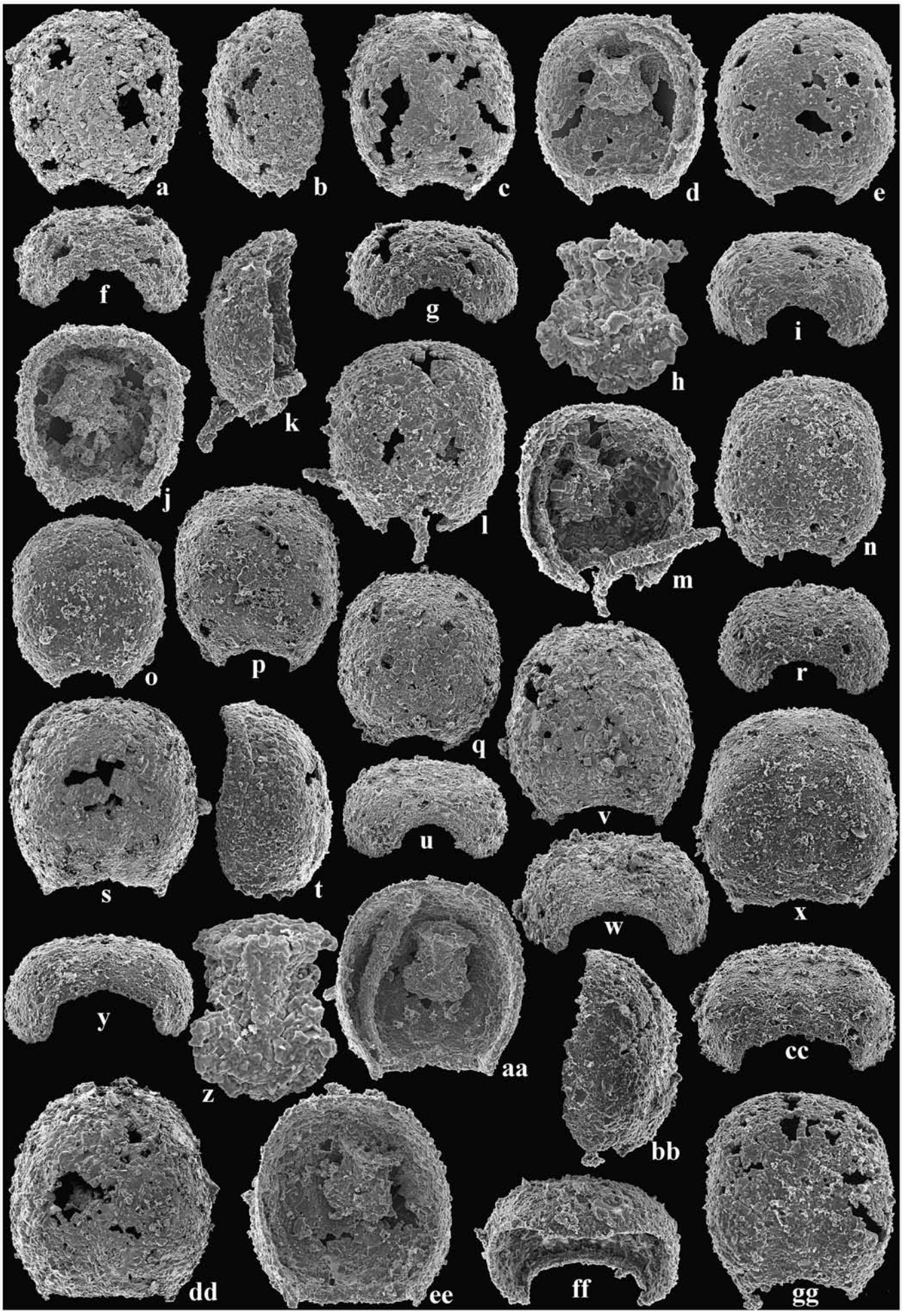

https://doi.org/10.1017/S026359330000122X Published online by Cambridge University Press

and protopygidium. However, no separation of somites representing the future protopygidium and cranidial border is recognised.

A few specimens of stage 2 have two furrows towards the back of the pleural region, the posterior of which is more weakly impressed (Fig. 7x, cc). In these specimens, the anterior furrow is the posterior cranidial border furrow and the posterior is the posterior cranidial marginal furrow. The very narrow (exsag.) region behind the posterior cranidial marginal furrow represents a differentiated protopygidium. This condition of the posterior region becomes much more conspicuous in protaspid stage 3 (Fig. 8e). In dorsal view, some specimens of stage 2 have a gently forward convex posterior margin (Fig. 7gg) whereas others have a gently bi-lobed posterior margin (Fig. 7x). The bi-lobed margin is found in stage 3. The presence of a bi-lobed margin in stage 2 indicates that the somite representing the protopygidium is already present.

Differentiation of a protopygidium occurs during protaspid stage 2 of *Bolaspidella housensis*, but it is not a conspicuous ontogenetic event that readily divides the protaspid period of *B. housensis* into 'anaprotaspid' and 'metaprotaspid' stages. Thus these terms are not employed in the present descriptions of the larvae of *B. housensis*. This observation provides an additional reason not to apply universally the terms 'anaprotaspid' and 'metaprotaspid' to all protaspid larvae (Chatterton & Speyer *in* Whittington *et al*. 1997; see also Edgecombe *et al*. 1988).

The spines developed along the lateral and posterior margins of protaspid hypostomes are later fused to form an undivided lateral and posterior border in the meraspid period. The spines are named 'hypostomal border spines'.

2.1. Description of ontogeny

Protaspid stage 1 (Figs 2a–d, 7a–r, u; Robison 1964, pl. 89, fig. 7). Exoskeleton without librigenae is sub-oval in outline; sagittal length (from anterior margin to indented posterior margin) ranges from 0·323 to 0·364 mm (0·342 mm in average, n=32) and transverse width ranges from 0·312 to 0·375 mm (0·343 mm on average, n=32); profile (in posterior and lateral view) is nearly flat on top (dorsally), and then steeply slopes laterally. Anterior pits are weakly developed in some specimens. Pair of short posterior fixigenal spines is located at back of exoskeleton (in dorsal view); fixigenal spines project from point above ventral most part of exoskeleton (in posterior and lateral views); and fixigenal spines are spaced close to each other (0·155 mm apart on average), and directed slightly inward and backward; spacing widens by factor of 0·14 (Fig. 5a) in this stage. Exoskeletal margin between spines is moderately concave backward (in dorsal view), and strongly arched dorsally (in posterior view). Facial suture is weakly sigmoidal (lateral view). Librigenae follow exoskeletal outline and almost reach back of exoskeleton; doublure is ornamented with fine terrace lines. Hypostome is shield-shaped; middle body is inverted elongated triangle in outline; nine border spines are present, anteriormost one with pointed end, and rest of them with blunted, shallowly bifurcated ends; and anterior border is strongly arched ventrally. Rostral plate is transversely elongated and of equal width to anterior margin of hypostome.

Protaspid stage 2 (Figs 2e–h, 7s, t, v-gg). Exoskeleton without librigenae is sub-oval in outline; it is 0·379 to 0·436 mm wide (0·404 mm in average, n=26), and 0·373 to 0·428 mm long (0·404 mm in average, n=26). Axial furrows are weakly impressed, and expand slightly forward (axial furrows are most conspicuous in posterior view; Fig. 7y, w, cc); occipital ring is weakly developed in some specimens; posterior end of axis, behind occipital ring, is poorly defined. Posterolateral ends of fixigenal area are relatively widely spaced (0·222 mm apart) and projected ventrally; spacing widens by factor of 0·22 (Fig. 5a); posterior fixigenal spines are blunt in some specimens, and absent in others. Posterior margin, between posterior fixigenal areas, is slightly indented forward sagittally or gently bi-lobed (in dorsal view), and moderately arched dorsally (in posterior view), forming transversely elongated pentagonal outline. Posterior cranidial border is weakly developed and anteriorly defined by weakly-impressed posterior cranidial border furrow in some specimens; posterior cranidial marginal furrow is very weakly impressed in others. Facial suture is moderately sigmoidal. Hypostomal and rostral plate morphologies are little changed from stage 1, except for size increase. Rostral plate is as wide (tr.) as anterior margin of hypostome (ventral view), and is much less arched ventrally than anterior hypostomal border.

Protaspid stage 3 (Figs 2i–l, 8, 9a, b, d, e, h, i; Robison 1964, pl. 89, fig. 6). Exoskeleton without librigenae is sub-oval to sub-rectangular in outline; it is 0·406 to 0·506 mm wide (0·465 mm in average, n=41) and 0·411 to 0·515 mm long (0·469 mm in average, n=41). Axial furrows expand moderately and shallow anteriorly; occipital ring is present. Cranidium occupies 86% (in average) of sagittal shield length; cranidial length increases at factor of 0·65 relative to exoskeletal length (Fig. 4c). Posterior cranidial border furrows reach lateral margin, and widen moderately and shallow distally. Facial sutures are strongly sigmoidal in lateral view, and curve relatively sharply dorsally near back. Back of librigena extends slightly behind back of fixigena (Fig. 8a, e); fine terrace lines occur on librigenal doublure, and extend to lower lateral portion of librigena (in lateral view; Fig. 8a). Posterior fixigenal areas are strongly projected ventrally, spaced 0·324 mm (in average) apart, and form transversely elongated rectangular outline; spacing increases by factor of 0·28 (Fig. 5a). Posterior cephalic marginal furrows are weakly developed, curve smoothly backward, and meet at upper lateral points of posterior exoskeletal margin (in posterior view). Protopygidium is transversely elongated, occupying 14% (average) of sagittal exoskeletal length; posterior sagittal margin is slightly indented anteriorly and dorsally. Hypostome is shield-shaped, and 0·182 mm (average) in sagittal length; anterior border is strongly arched ventrally. Rostral plate is narrower (tr.) than anterior margin of hypostome.

Two specimens display partial separation between cranidium and protopygidium (Fig. 9a, b, d, e, h, i). Their plots

Figure 7 SEM photographs of protaspid stages 1 and 2 of *Bolaspidella housensis* (Walcott, 1886). All figures are × 100, unless otherwise noted. All specimens are from the Marjum Formation. (a, b, f, j) protaspid stage 1, UA 13475: (a) dorsal view; (b) lateral view; (f) posterior view; (j) ventral view; note the attached librigenae and detached hypostome. (c, d, g, h) protaspid stage 1, UA 13476: (c) dorsal view; (d) ventral view; note that anterior border of detached hypostome is strongly arched ventrally; (g) posterior view; (h) magnified view of hypostome, × 200; although poorly preserved, nine hypostomal border spines are recognised. (e, i) protaspid stage 1, UA 13477: (e) dorsal view; (i) posterior view; note that posterior fixigenal spine located above ventral ends of posterior fixigenal area. (k, l, m) protaspid stage 1, UA 13478: (k) lateral view; (l) dorsal view; (m) ventral view. (n, r) protaspid stage 1, UA 13479: (n) dorsal view; (r) posterior view. (o) protaspid stage 1, UA 13480, dorsal view. (p) protaspid stage 1, UA 13481, dorsal view. (q, u) protaspid stage 1, UA 12772. (q) dorsal view; (u) posterior view. (s, t, y, z, aa) protaspid stage 2, UA 13482: (s) dorsal view; note that posterior half of left librigena is attached and the anterior half is detached; (t) lateral view; (y) posterior view; (z) magnified view of hypostome and slightly displaced rostral plate, × 200; (aa) ventral view. (v, w) protaspid stage 2, UA 13483: (v) dorsal view; (w) posterior view; (x, cc) protaspid stage 2, UA 13484: (x) dorsal view; (cc) posterior view; (bb, gg) protaspid stage 1, UA 13485: (bb) lateral view; (gg) dorsal view; (dd, ee, ff) protaspid stage 2, UA 13486: (dd) dorsal view; (ee) ventral view; (ff) anterior ventral view.

https://doi.org/10.1017/S026359330000122X Published online by Cambridge University Press

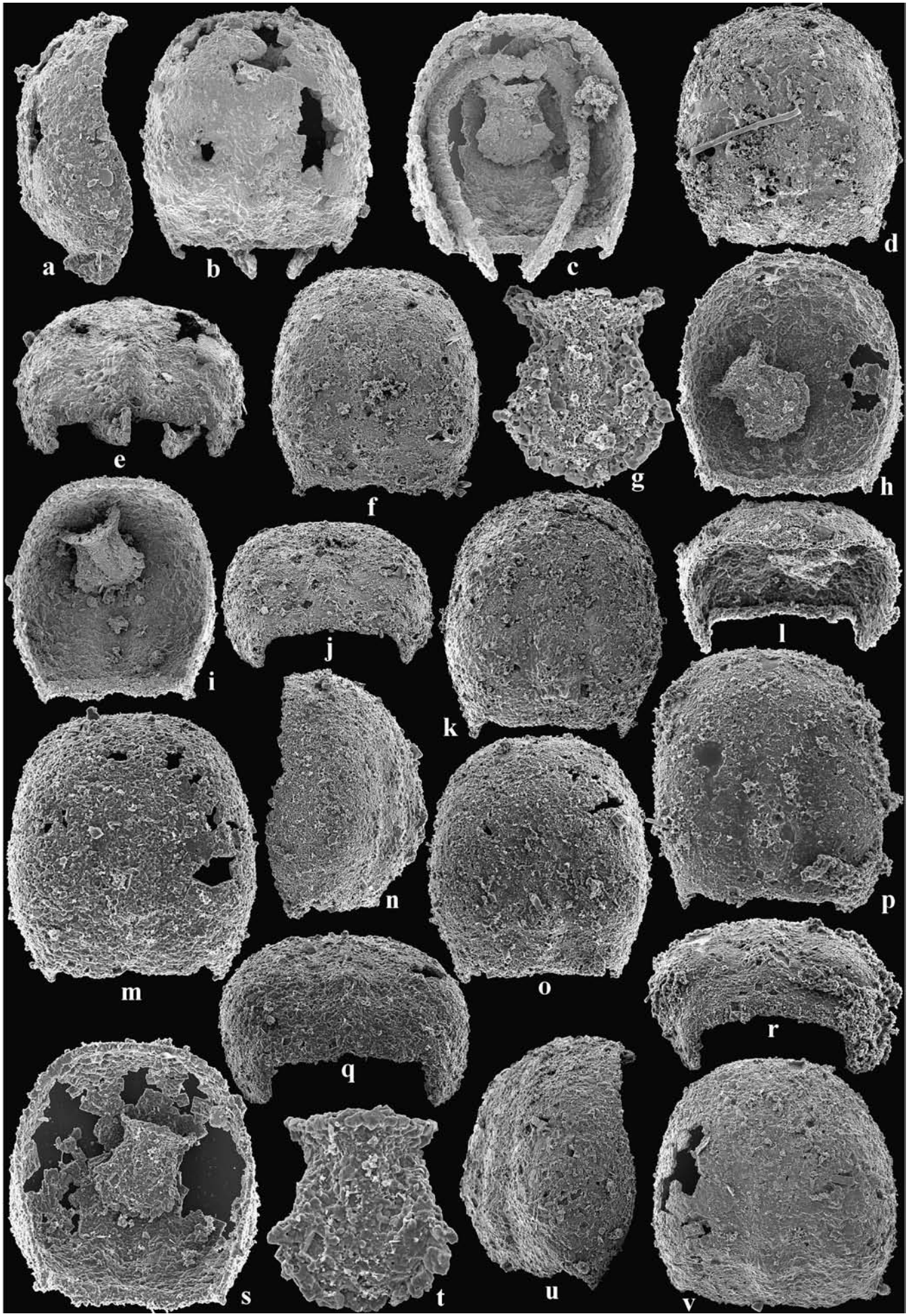

https://doi.org/10.1017/S026359330000122X Published online by Cambridge University Press

of length versus width fall within cluster of protaspid stage 3 (Fig. 4a). Apparent separation develops only in middle (axial) portion of shield. They may represent fossilised inter-molting stage, when weakness along boundary between cranidium and transitory pygidium began to develop.

Meraspid degree 0 (Figs 2m–p, 9c, f, g, j–l). Two articulated specimens were recovered. Exoskeleton is sub-oval in outline, with flattened top and steep lateral portions (posterior view). Cranidium is between 0·451 and 0·468 mm, and transitory pygidium is between 0·160 and 0·207 mm in sagittal length. Axial furrows are moderately wide and deep. Occipital ring has highest convexity of cephalic axis, and is slightly protruded backward (lateral view). Posterior lateral end of fixigena turns down so that it is lower than transitory pygidium (posterior view). Librigenae have two or three weakly impressed terrace lines on lower lateral portion, and on ventral doublure. Hypostomal border is spinose; and is 0·239 mm in sagittal length in UA 12778 (Fig. 9k). Transitory pygidium is oriented horizontally (in lateral and posterior views), with lateral and posterior margins ornamented by two to three short saw-tooth shaped spines.

Meraspid degree 1 (Figs 2q–t, 9m–p, 11a, e). One articulated specimen was recovered. Glabella slightly expands forwards. Axial furrows are moderately deep near posterior half of cranidium, but shallow forward and are inconspicuous near front of cranidium. Posterior cranidial border furrows are deep and widen distally, not reaching librigenae; anterior slope of furrow is steep and posterior slope is gentle. Librigenae are elongate blade-shaped, and posteriorly extend behind back of fixigenal area by developing pair of stout librigenal spines; fine terrace lines occur on ventral doublure, and extend into lower lateral portion of librigenae. Hypostomal border is spinose; anterior border is strongly arched ventrally. Rostral plate is flat horizontally; anterior margin is slightly narrower (tr.) than anterior hypostomal margin, and posterior margin is about quarter of width of anterior hypostomal margin, forming inverted trapezoid. Transitory pygidium has three short saw-tooth shaped marginal spines and three axial rings; pleural furrows are weakly impressed.

Meraspid degree 2 (Figs 10a–c, 11b, c; Robison 1964, pl. 89, fig. 5). Two incompletely articulated specimens were recovered. Pleural and interpleural furrows in transitory pygidia are more deeply impressed than in meraspid stage 1. Robison (1964, pl. 89, fig. 5) assigned a meraspid cranidium to meraspid degree 0. Compared to the cranidium of the articulated meraspid degree 0 (Fig. 9c, f, g, j–l), the cranidium is less circular in outline. It is more similar to the cranidia of meraspid degree 2.

Meraspid degree 3–4 (Fig. 10d, g; Robison 1964, pl. 89, fig. 4). Cephalon is semi-ovoid in outline. Anterior border is differentiated, and is delimited posteriorly by nearly straight border furrow. Glabella forms elongate rectangle. Palpebral lobes are small, and defined adaxially by shallow palpebral furrows. Occipital spine is short and stout. Librigenal spine is one-third of cranidial length; ventral doublure is ornamented by fine terrace lines. Hypostomal border is entire.

Meraspid degree 5 (Fig. 10e, f, d; Robison 1964, pl. 89, fig. 3). Palpebral furrow is straight. Palpebral lobe is slightly convex laterally. Four pairs of tubercles are present on glabella, and tubercle is present on posterior pleural bands of thoracic segment at mid-thoracic length. Fourth and fifth (from anterior) thoracic segments have short axial spine; anterior three thoracic segments do not have axial spine. Anterior three pygidial segments have axial spine.

Meraspid degree 6–7 (Figs 3a–c, 10h–j, l–n, q, s). Anterior cranidial border furrow is wide and deep. Three pairs of tubercles are developed on fixigenal fields; anterior pair is slightly anterior to mid-glabellar length, middle pair is opposite third (from anterior) paired tubercles on glabella, and posterior pair is slightly anterior to posterior cranidial border furrows. Librigenal spines are half of cranidial length; posterior tip is slightly curved outward. Ventral doublure is covered by fine terrace lines. Metamerically repeated row of tubercles occurs on posterior pleural bands of thoracic segments, in position of fulcrum, continuing onto transitory pygidium. Hypostomal anterior border is strongly arched ventrally; and it is estimated that anterior hypostomal margin is much longer than posterior margin of rostral plate. Posterior three thoracic segments and anterior two pygidial segments have short, stout axial spine. Transitory pygidium has four or five axial rings and pleural segments; posterior margin is dorsally arched (in posterior view). Some individuals are enrolled.

Meraspid degree 8 (Fig. 10k, r, t, u). Anterior border furrow is curved slightly backward sagittally, indicating commencement of plectral stage. Palpebral lobe is moderately convex laterally. No axial spine is present on transitory pygidium; all segments with axial spine have been released into thorax.

Meraspid degree 9 and subsequent stages (Figs 10o, p, 11f–w; Robison 1964, pl. 88, figs 16–21, pl. 89, figs 1, 2, 8–11). Occipital spine is slender and long. Preglabellar field is differentiated. Cranidial and librigenal surfaces are covered by fine granules: tubercles on cranidial surface, that are conspicuous in previous stages, disappear. Two pairs of glabellar furrows are present; one pair, representing anteriormost pair, is added in later stages. Posterior facial sutures deeply cut into cranidium and run transversely in later stages. Hypostomal anterior border is slightly curved ventrally (in posterior view). Pygidium is sub-elliptical in outline; posterior margin is slightly indented sagittally forwards (dorsal view), and moderately arched dorsally (in posterior view). Robison (1964, pl. 89, fig. 11) illustrated a complete holaspid specimen, with 15 thoracic segments.

Remarks on ontogeny. Robison (1964, pl. 88, figs 6, 7) illustrated two protaspid specimens of *Bolaspidella housensis* from the Marjum Formation, and designated anaprotaspid and metaprotaspid stages, respectively. The smaller one (fig. 7) is 0·338 mm wide and 0·354 mm long (measurements are based on his illustration). This falls within the cluster of the length versus width plots of the present protaspid stage 1. All the observable morphological features agree with the features of protaspid stage 1. The larger specimen figured by Robison (1964, pl. 88, fig. 6) was assigned to the metaprotaspid stage. Robison (1964, p. 555) stated, 'The protopygidium is not clearly separated from the protocranidium, except at the posterior end of the occipital ring'. This indicates that it may correspond to the two probably intermolting specimens between protaspid stage 3 and meraspid degree 0 (Fig. 9a, b, d, e, h, i). The size of the specimen (0·477 mm wide and 0·5 mm long) fits into protaspid stage 3 (Fig. 4a).

Figure 8 SEM photographs of protaspid stage 3 of *Bolaspidella housensis* (Walcott, 1886). All figures are × 100, unless otherwise noted. All specimens are from the Marjum Formation. (a, b, c, e) UA 12777: (a) lateral view; (b) dorsal view; (c) ventral view; (e) posterior view; note that posterior end of librigenae is hook-shaped. (d, g, h, l) UA 13487: (d) dorsal view; (g) magnified view of hypostome, × 200; (h) ventral view; (l) anterior ventral view. (f, i, j) UA 12774: (f) dorsal view; (i) ventral view; (j) posterior view. (k) UA 12775, dorsal view. (m, n, q) UA 12776: (m) dorsal view; (n) lateral view; (q) posterior view. (o) UA 13488, dorsal view. (p, r) UA 13489: (p) dorsal view; (r) posterior view. (s, t) UA 13490: (s) ventral view; (t) magnified view of hypostome, × 200; note the presence of nine hypostomal border spines. (u, v) UA 13491: (u) lateral view; (v) dorsal view.

https://doi.org/10.1017/S026359330000122X Published online by Cambridge University Press

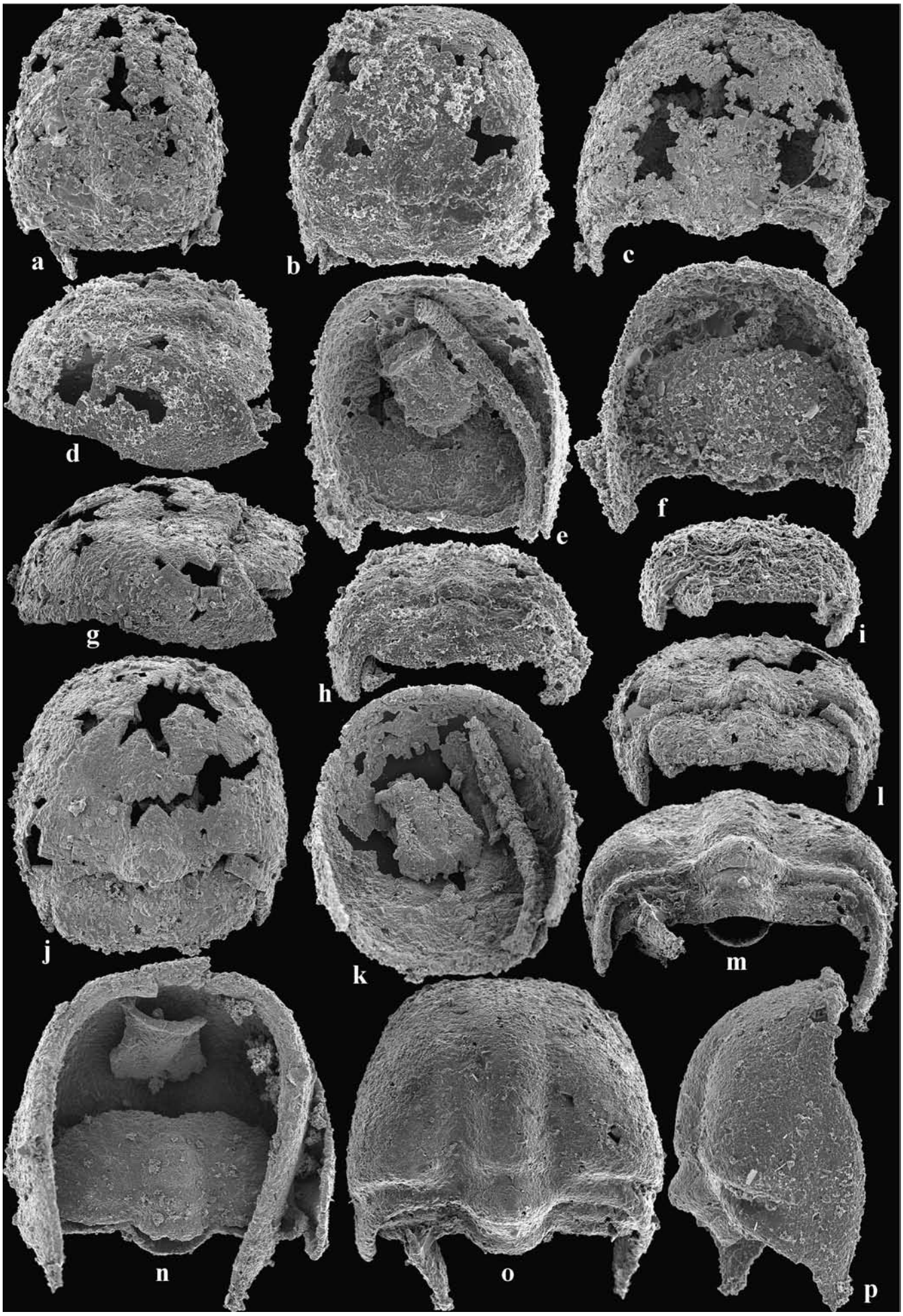

https://doi.org/10.1017/S026359330000122X Published online by Cambridge University Press

The rostral plate displays an interesting ontogenetic trend in terms of the transverse length of its posterior margin. The plate remains rectangular and the posterior margin is as long as the hypostomal anterior border until meraspid degree 0. The rostral plate of meraspid degree 1 (Fig. 9n) has a short (tr.) posterior margin, resulting in an inverted trapezoidal outline. This trend appears to continue into meraspid degree 6. Upon the basis of the estimated distance between the anterior proximal ends of the two displaced free cheeks, the rostral plate of meraspid degree 6 (Fig. 10m) is inferred to have almost the form of an inverted triangle. However, this trend of reduction in width (tr.) of the posterior margin of rostral plate is reversed in later ontogenetic stages. The rostral plate of an adult specimen illustrated by Robison (1964, pl. 88, fig. 19) shows that the posterior margin is about three-quarters of the width of the hypostomal anterior border, and the anterior margin remains as wide as the hypostomal anterior border. The width of the posterior margin of the rostral plate appears to be progressively increased with respect to the width of hypostomal anterior border, sometime after meraspid degree 6. It is rare for such allometric trends to be reversed during the ontogeny of a single species.

Ptychopariide sp. A
(Fig. 12a–m)

Description of protaspides. Exoskeleton is sub-circular, and ranges from 0·301 to 0·363 mm in width and 0·267 to 0·322 mm in length (n=20); lateral profile is flattened on top and gently sloping distally. Posterior margin is moderately convex forward (in dorsal view), and strongly arched dorsally (in posterior view). Anterior pits are moderately impressed. Anteriormost axial lobe forms inverted triangle, and is weakly defined by axial furrows. Pair of posterior fixigenal spines is slender, pointed inward, and spaced 0·113 mm apart (in average). Facial sutures are straight. Librigenae reach mid-length of exoskeleton. Hypostome is shield-shaped, with elongated triangular median body and nine spines along lateral and posterior borders. Rostral plate is as wide as anterior margin of hypostome.

Remarks. These protaspid specimens could represent the earliest stage of *Bolaspidella housensis*. However, the present authors have provided, above, reasons for not assigning these specimens to that species.

Ptychopariide sp. B
(Figs 3h, i, 12q, r, s, v, x)

Description of protaspides

Protaspid stage 1 (Fig. 12q, r). Exoskeleton is circular; it is 0·356 mm wide and 0·305 mm long. Anterior pits are moderately impressed. Three pairs of short fixigenal spines are present; anterior pair is located around mid-shield length; mid-fixigenal pair is at posterior one-seventh of sagittal exoskeletal length; and posterior pair is spaced 0·094 mm apart. Librigenae extend back to opposite anterior fixigenal spine pair.

Protaspid stage 2 (Figs 3h, i, 12s, v, x). Exoskeleton is circular; it is 0·454 to 0·474 mm in width and 0·384 to 0·410 mm in length (n=5). Anterior pits are well impressed. Anteriormost axial lobe forms inverted triangle. Three pairs of short fixigenal spines are present; and posterior pair is spaced 0·163 mm apart (in average). Shield-shaped hypostome has nine border spines.

Remarks. The possible association of protaspid stage 2 of this species with protaspides of ptychopariide sp. A is refuted (see above) by the discovery of a protaspid stage 1 specimen with three pairs of fixigenal spines (Fig. 12q, r).

Ptychopariide sp. C
(Figs 3l, m, 12n, o, t, u)

Description of protaspides. Exoskeleton has slightly backward tapering sub-oval outline. Four specimens were obtained; they are 0·363 to 0·481 mm wide and 0·352 to 0·429 mm long. Posterior fixigenal spines are long and slender, and spaced 0·102 mm apart. Librigena is one-third of shield length. Hypostome has nine border spines; except for anteriormost one, spines are separated by narrow gaps; lateral margin is relatively strongly curved inwards. Rostral plate is transversely elongated, and wider than anterior hypostomal margin.

Remarks. These protaspides differ from other co-occurring protaspides in having a backward-tapering exoskeleton, a well-defined anterior axial lobe and blunt hypostomal border spines that are separated by very narrow slots.

Ptychopariide sp. D
(Figs 3j, 12y, cc)

Description of protaspides. Exoskeleton sub-elliptical in outline; 0·411 to 0·481 mm wide and 0·454 to 0·507 mm long. Anterior pits relatively weakly impressed; axial furrows moderately impressed in anterior axial portion and shallow out to be absent posteriorly. Posterior cranidial marginal furrows are weakly impressed.

Remarks. These protaspid specimens are similar to those of *Syspacheilus dunoirensis* (Hu 1972). Robison (1964) reported the occurrence of three *Modocia* species from the same zone as *Bolaspidella housensis*. Robison (1964, 1988) included *Modocia* and *Syspacheilus* in the family Marjumiidae. This may indicate that their protaspides are similar to each other. These protaspides could belong to *Modocia*. The association needs to be further assessed upon the basis of more material.

Order Corynexochida Kobayashi, 1935
Corynexochide sp. A
(Figs 3k, 12w, z-bb)

Description of protaspides. Exoskeleton is sub-hexagonal to sub-circular in outline; it is 0·500 to 0·549 mm wide and 0·388 to 0·468 mm long (n=3). Anterior pits are strongly impressed, and connected with axial-sagittal furrow. Sagittal furrow is impressed up to mid-shield length and then disappears. Three pairs of fixigenal spines are present; anterior pair is located at mid-shield length and mid-fixigenal pair is at one-eighth of shield length; posterior pair is parallel, and spaced 0·187 mm (average) apart.

Figure 9 SEM photographs of protaspides and meraspides of *Bolaspidella housensis* (Walcott, 1886). All figures are × 100. All specimens are from the Marjum Formation. (a, d, i) UA 13492: (a) dorsal view; (d) lateral view; (i) posterior view. (b, e, h) UA 13493: (b) dorsal view; (e) ventral view; note the presence of detached left librigena and hypostome and that rostal plate is transversely narrower than anterior margin of hypostome; (h) posterior view. (c, f) meraspid degree 0, UA 13494: (c) dorsal view; (f) ventral view. (g, j, k, l) meraspid degree 0, UA 12778: (g) lateral view; (j) dorsal view; (k) ventral view; note that hypostomal border spines are still present. (l) posterior view. (m, n, o, p) meraspid degree 1, UA 12780: (m) posterior view; (n) ventral view; note that posterior margin of rostral plate is much narrower than anterior margin of hypostome; (o) dorsal view; (p) lateral view; note the outline of facial suture.

https://doi.org/10.1017/S026359330000122X Published online by Cambridge University Press

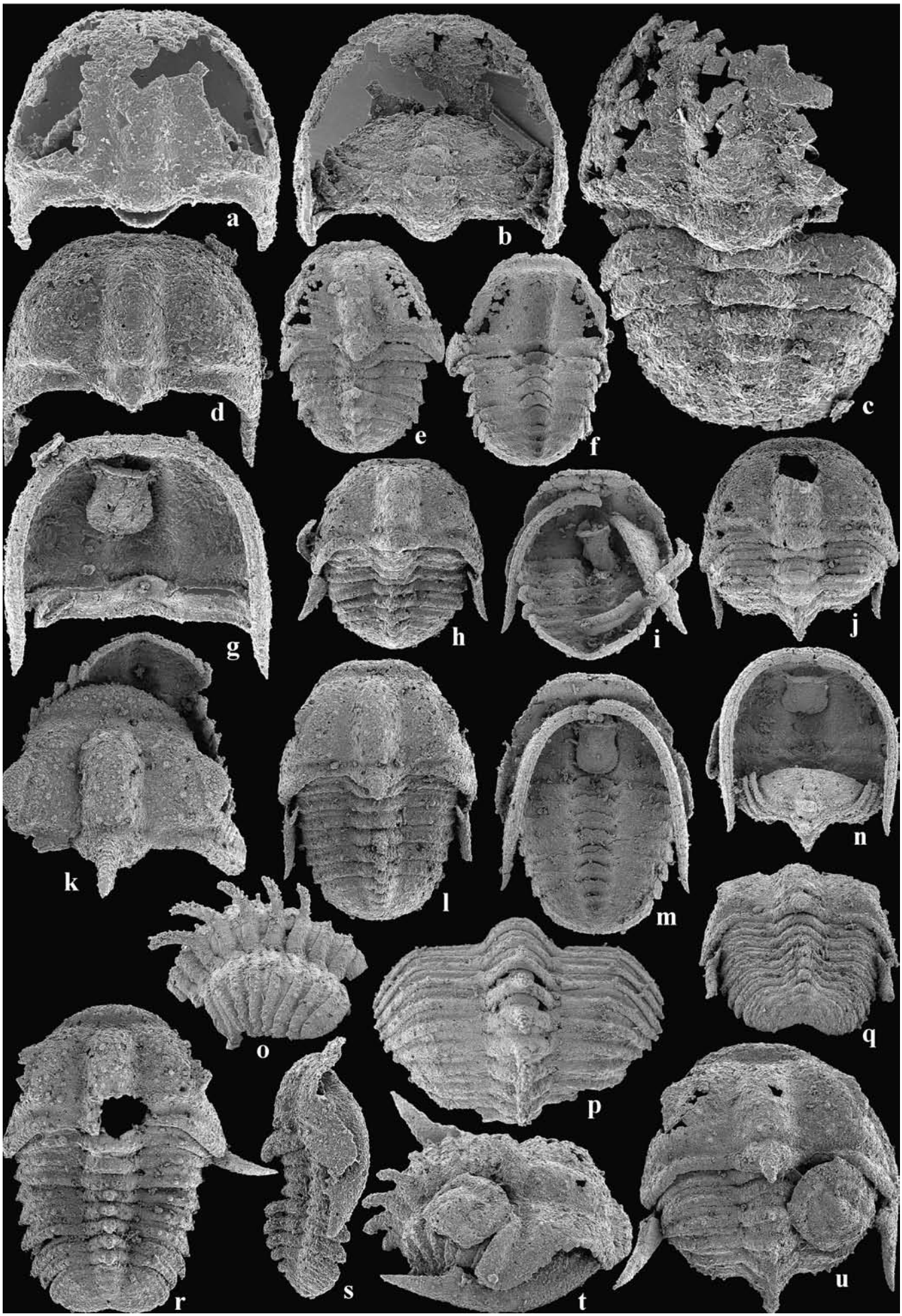

https://doi.org/10.1017/S026359330000122X Published online by Cambridge University Press

Remarks. These specimens are similar to those of *Leiostegium* and other corynexochide protaspides (Lee & Chatterton 2003) in having a sub-hexagonal outline and sagittal furrow. Robison (1964) reported the occurrence of a few corynexochide taxa from the same rock unit (e.g., *Bathyuriscus*, *Holteria*, *Olenoides*, and so on) with which these protaspides could be associated.

3. Upper Cambrian protaspides similar to those of *Bolaspidella housensis*

Glaphyraspis parva (Walcott, 1899)
(Figs 3n–q, 13a–t, v, x, y)

1899 *Liostractus parva* Walcott, p. 463, pl. 65, fig. 6.
1937 *Glaphyraspis parva*, Resser, p. 12.
1971 *Glaphyraspis parva*, Hu and Tan [part], p. 66, pl. 9, figs 4–10, 11–33 [only].
1992 *Glaphyraspis parva*, Pratt, p. 71, pl. 26, figs 13–22 (see for synonymy to date).

Holotype. A cranidium from Upper Cambrian rocks, Wyoming (Walcott 1899, pl. 65, fig. 6).

Diagnosis. See Pratt (1992, p. 71) for holaspid diagnosis.

Occurrence of materials described herein. Silicified materials (Fig. 13a–k, m–o, q, r, v) from the *Aphelaspis* Zone (lowermost Steptoean) of Dunderberg Formation, McGill section, east-central Nevada (Fig. 1). Crack-out specimens from *Aphelaspis* Zone of Deadwood Formation, Moll Section, Bear Butte, southeastern Deadwood City, northern Black Hills, South Dakota (Hu & Tan, 1971; see also Fig. 1).

Association of protaspides. Hu & Tan (1971) documented the ontogeny of *Glaphyraspis parva* occurring in the Deadwood Formation. They associated several protaspid specimens with this species. The protaspid specimens were re-examined by Lee (2002) where a detailed account for the association can be found. It cannot be claimed with confidence that some poorly preserved specimens (Lee 2002, pl. II-9, figs 1–7) belong to the same ontogeny. However, a gradual morphological transformation, observed across a number of ontogenetic stages (Lee 2002, pl. II-9, figs 8–26; see also Hu & Tan 1971, pl. 9, figs 4–33), represented by well-preserved specimens confirms that the association is correct.

Silicified specimens of *Glaphyraspis ornata*, occurring in the Dunderberg Formation, Nevada were described by Palmer (1962); *G. ornata* was synonymised under *Glaphyraspis parva* by Pratt (1992). New specimens were collected by the authors from the same locality. A striking similarity is found between crack-out specimens from the Deadwood Formation and the silicified specimens, (compare Fig. 13b and s). This lends additional support for the assignment of protaspid specimens from the Deadwood Formation to *G. parva*. Comparison of silicified and crack-out materials illustrates that it is more difficult to obtain complete morphological information from crack-out materials. In particular, the ventrally projected exoskeletal parts such as posterior fixigenal spines and ventrally projected ends of posterior fixigenal area are difficult to observe in crack-out specimens (compare Fig. 13m and y). Two protaspid stages are recognised (Fig. 6c).

3.1. Description of ontogeny

Protaspid stage 1 (Fig. 13a, f, g). Exoskeleton is sub-circular; it is 0·285 to 0·294 mm wide (0·288 mm in average, n=3) and 0·256 to 0·291 mm long (0·274 mm in average, n=3). Axis expands forward. Posterior fixigenal spines are spaced 0·158 mm apart, and located at about middle of lateral profile height (posterior view). Posterior ends of librigenae reach anterior one third of sagittal exoskeletal length. Posterior margin is broadly indented (dorsal view) and strongly arched to form trapezoidal outline (posterior view).

Protaspid stage 2 (Fig. 13b, c, h, i, m, o, q–t, y; Palmer, 1962, pl. 19, figs 16, 17). Exoskeleton is sub-rectangular to sub-oval; it is 0·342 to 0·395 mm wide (0·362 mm in average, n=9), and 0·345 to 0·373 mm long (0·350 mm in average, n=9). Cranidium is 0·301 mm in length (sag.), occupying 86% of exoskeletal length. Forward-expanding axis has four glabellar lobes that are delineated by weakly impressed transglabellar furrows; axial furrows shallow forward. Posterior cranidial border furrows almost reach lateral exoskeletal margin distally. Posterior cephalic marginal furrows are shallow and narrow. Posterior fixigenal area ventrally extends far below protopygidium (in posterior view). Posterior fixigenal spines are spaced 0·229 mm apart, and located well above ventral end of posterior fixigenal area (in posterior view). Facial sutures reach anterior one-third of sagittal exoskeletal length. Rostral plate is present. Protopygidium is small (sagittal length 14% of sagittal exoskeletal length), with one axial ring.

Meraspid degree 0 (Fig. 13d, e, j, k; Palmer, 1962, pl. 19, fig. 15). Two specimens were recovered. Exoskeleton is sub-oval; and is 0·356 to 0·363 mm wide and 0·359 to 0·366 mm long. Cranidium is 0·314 mm in sagittal length. Posterior fixigenal spines are spaced 0·225 mm apart. Protopygidium has two axial rings, and is inverted sub-trapezoid in shape.

Remarks. Palmer (1962, pl. 19, fig. 16) illustrated an 'anaprotaspis'. This specimen differs from protaspid stage 1 described herein in having a sub-rectangular exoskeleton that is the same as that of protaspid stage 2. Thus, it is assigned here to protaspid stage 2.

Two specimens were recovered that show a clear separation between the cephalon and the protopygidium; the ventral illustration (Fig. 13e) clearly demonstrates the separation. These two specimens are assigned to meraspid degree 0, even though their length and width plots fall within those of protaspid stage 2 (Fig. 6c). These two individuals seem to have matured faster in the timing of onset of the meraspid period than other individuals that still belong to protaspid stage 2.

Ptychopariide sp. E
(Figs 3r–t, 13u, w, x, z, aa–ee)

1971 *Apomodocia conica* Hu [part], p. 88, pl. 9, figs. 3, 5–19 [only].

Occurrence of materials described herein. This species occurs in *Cedaria* zone (Upper Cambrian). The materials were

Figure 10 SEM photographs of meraspides of *Bolaspidella housensis* (Walcott, 1886). All specimens are from the Marjum Formation. (a, b) enrolled meraspid degree 2, UA 13495: (a) dorsal view, × 100; (b) ventral view, × 100; (c) meraspid degree 2, UA 12817, dorsal view, × 100. (d, g) cephalon with one thoracic segment of meraspid degree 3 or 4, UA 12781: (d) dorsal view, × 50; (g) ventral view, × 50: note that the hypostomal border is entire. (e, f) meraspid degree 5, UA 13496: (e) dorsal view, × 30; (f) ventral view, × 30. (h, i) meraspid degree 6, UA 13497: (h) dorsal view, × 30; (i) ventral view, × 30; (j, n) partially enrolled meraspid degree 7, UA 12782. (j) dorsal view, × 30. (n) ventral view, × 30. (k) enrolled meraspid degree 8, UA 13498, dorsal view, × 30. (l, m, q, s) meraspid degree 6, UA 12783: (l) dorsal view, × 30; (m) ventral view, × 30; (q) oblique posterior view, × 30; (s) lateral view, × 30. (o, p) enrolled 9 thoracic segments, UA 12792: (o) lateral view, × 30; (p) dorsal view, × 30. (r) meraspid degree 8, UA 12786, dorsal view, × 30. (t, u) enrolled meraspid degree 8, UA12784: (t) lateral view, × 30; (u) dorsal view, × 30.

https://doi.org/10.1017/S026359330000122X Published online by Cambridge University Press

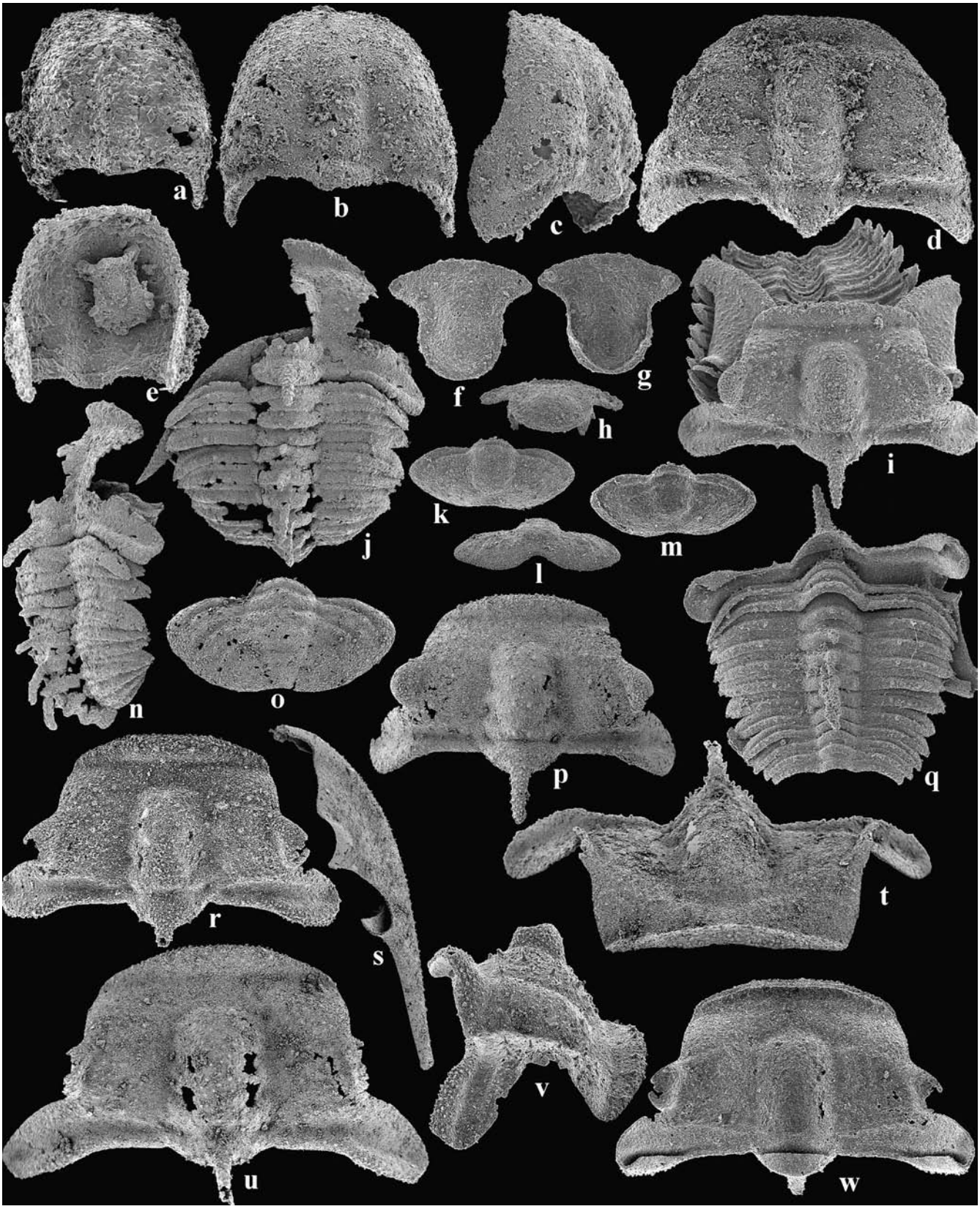

Figure 11 SEM photographs of meraspides and holaspides of *Bolaspidella housensis* (Walcott, 1886). All specimens are from the Marjum Formation. (a, e) cranidium of meraspid degree 1, UA 13499: (a) dorsal view, × 75; (e) ventral view, × 75. (b, c) cranidium of meraspid degree 2, UA 12779: (b) dorsal view, × 75; (c) ventral view, × 75. (d) cranidium of meraspid degree 5, UA 12787, × 50. (f–h) holaspid hypostome, UA 13500: (f) ventral view, × 25; (g) dorsal view, × 25; (h) posterior view, × 25. (i, q) meraspid specimen with 12 thoracic segments, UA 13501: (i) top view, × 20; (q) bottom view, × 20. (j, n) meraspid specimen with 10 thoracic segments, UA 12791: (j) dorsal view, × 20; (n) lateral view, × 20. (k–m) holaspid pygidium, UA 13502: (k) dorsal view, × 20; (l) posterior view, × 20; (m) ventral view, × 20. (o) holaspid pygidium, UA 12793, dorsal view, × 20. (p) late meraspid cranidium, UA 12788, dorsal view, × 20. (r, v, w) late meraspid cranidium, UA 13503: (r) dorsal view, × 20; (v) oblique lateral view, × 20; (w) ventral view, × 20. (s) late meraspid free cheek, UA 12790, dorsal view, × 20. (t, u) holaspoid cranidium, UA 12789: (t) anterior view; × 20. (u) dorsal view, × 20.

https://doi.org/10.1017/S026359330000122X Published online by Cambridge University Press

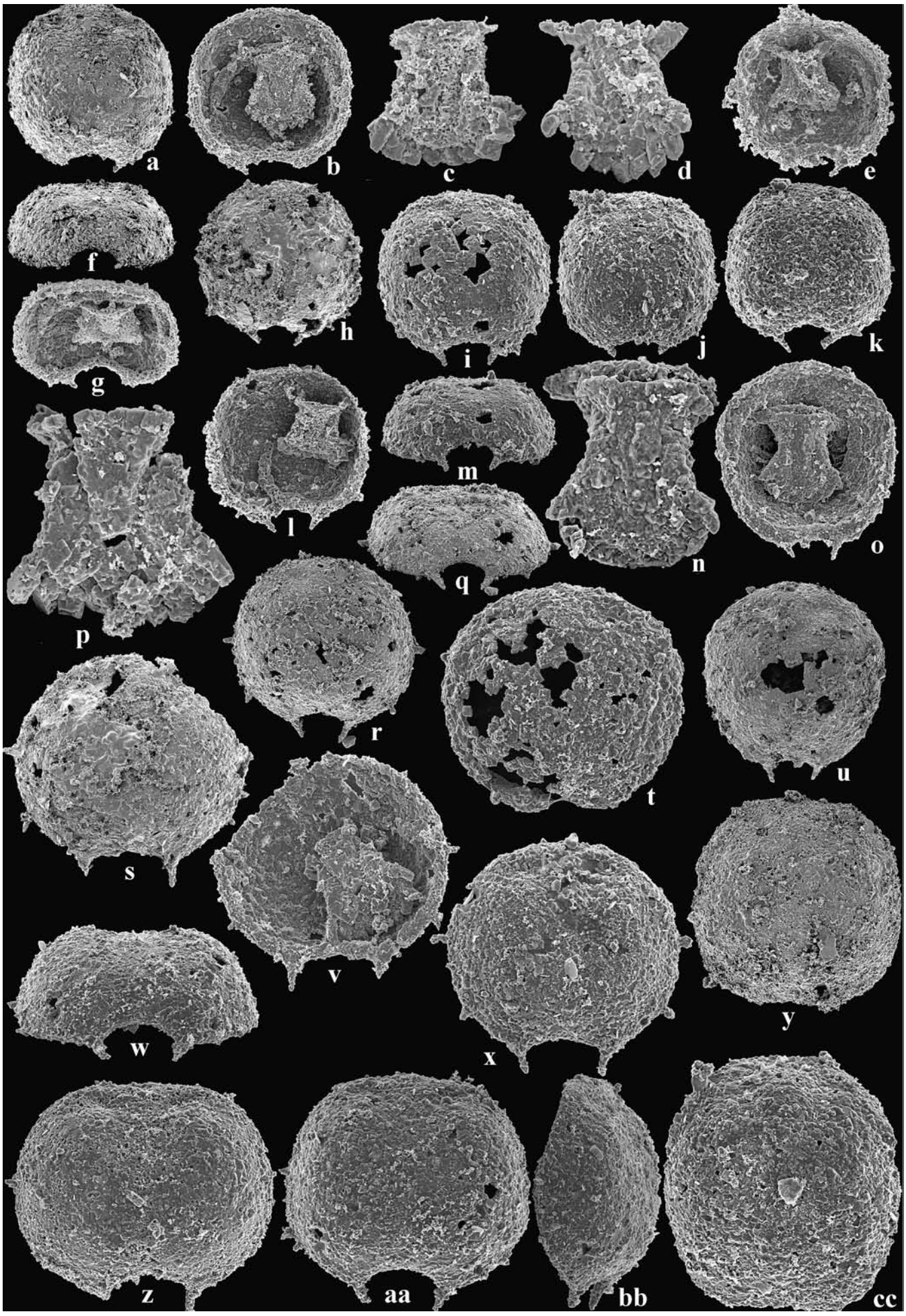

https://doi.org/10.1017/S026359330000122X Published online by Cambridge University Press

recovered from a locality near Wasatch Mountain, Utah, U.S.A. (Fig. 1).

Association of protaspides. Hu (1971) described several protaspides from an unknown locality near Wasatch Mountain, Utah, U.S.A., and assigned them to a new species, *Apomodocia conica* (Fig. 13x, ee). Re-examination of these protaspides reveals that they include several distinct morphotypes that belong to different ontogenies (see Lee (2002) for additional details). Three of these specimens (Fig. 13u, w, z, aa–dd), assigned herein to Ptychopariide sp. E, are considered to represent part of the ontogeny of a single species. They are characterised by having ventrally projected posterior ends of the fixigenae. However, it is difficult to assign them to *A. conica*, because the morphological transition from the largest protaspid specimen (Fig. 13bb, cc) into the smallest cranidium (Hu 1971, pl. 9, fig. 9) does not seem to be as continuous as would be expected in the ontogeny of a single species. It would require changing a parallel-sided axis with a forward-expanding anterior part into a forward-tapering glabella, a straight into a rounded anterior margin, and a strongly curved into a transversely straight posterior cranidial margin. Should they belong to the ontogeny of a single species, these changes would have to be explained as a result of a radical metamorphosis that occurred between the protaspid and meraspid periods. In addition, the meraspid cranidia that were assigned to *A. conica* (Hu 1971, pl. 9, figs 9–11) are indistinguishable from those of *Cedarina cordillerae* (Lee 2002, pl. II-11, figs 9–11) a species recovered from the same locality (Hu 1971). It seems most likely that the meraspid cranidia belong to the ontogeny of *C. cordillerae*. Upon the basis of the materials available at present, it cannot be assessed whether or not these protaspid specimens belong to the ontogeny of *A. conica*.

3.2. Description of protaspides

Protaspid stage 1 (Fig. 13u, z, dd). Exoskeleton is rectangular; it is 0·405 mm long and 0·375 mm wide. Axis is parallel-sided, with forward-expanding anteriormost lobe; anterior pits are relatively well impressed; axial furrows are weakly-impressed. Posterior margin is slightly indented anteriorly at its sagittal portion (in dorsal view) and arched dorsally (in posterior view). Posterior ends of posterior fixigenal area are relatively long and projected ventrally and backward.

Protaspid stage 2 (Fig. 13w, aa–cc). Two specimens are re-described. Exoskeleton is sub-rectangular; it is 0·531 mm wide and 0·557 mm long; exoskeleton is wide and flat on top, and slopes steeply laterally (in posterior view). Axis is parallel-sided, with rapidly forward-expanding frontal lobe, occupying 25% of exoskeletal width. Posterior cranidial marginal furrows run transversely almost half distance to margin and then turn backward at 45° angle. Posterior fixigenal area projects below protopygidium in posterior view. Protopygidium has two or three axial rings, and occupies 22% of exoskeletal length; posterior margin is slightly indented.

4. Implications of protaspid similarities

Protaspides of *Bolaspidella housensis* are similar to those of *Glaphyraspis parva* and Ptychopariide sp. E. Protaspid stage 1 of *B. housensis* is most similar to the protaspid stage 2 of *G. parva*, and protaspid stage 3 of *B. housensis* is similar to the protaspid stage 2 of Ptychopariide sp. E; each pair is similar in size. In particular, a gently forward-expanding axis and a ventrally projected fixigenal area, in posterior view, are observed in all these protaspides. By contrast, holaspid morphologies of these species are not as similar to each other; the holaspid similarities can only be accommodated within a generalised ptychopariide morphology. A simple, well-known pattern is observed in that similar earlier ontogenetic stages of two taxa grow into dissimilar later ontogenetic stages. This pattern has been documented in the development of a number of living taxa as well as in ontogenies of several trilobite taxa. It is translated into a taxonomic statement that a particular earlier developmental form is a diagnostic feature of a respective higher taxon, e.g., the pharyngular stage of vertebrates and the nauplius larva of crustaceans. The concept of a 'phylotypic stage', when all members of a higher taxon show a maximum degree of morphological similarity (Slack *et al.* 1993), appears to be an equivalent statement. This statement has been interpreted as a phylogenetic statement, that similarity in early ontogenetic stages provides evidence of common ancestry. Chatterton & Speyer (*in* Whittington *et al.* 1997, p. 211) stated, 'As a rule, monophyletic groups based on characteristics of adult growth stages have similar larvae, . . . so that larval morphology appears to be a useful indicator of relationship. . . . Some synapomorphies visible only in larval stages may be used to recognise and define large groups of trilobites'. These statements imply that morphological information provided by earlier ontogenetic stages such as trilobite protaspides is informative, maybe more informative than later ontogenetic stages in some cases, for defining a natural group.

The recent classification schemes (for example, Pratt 1992) state that *Bolaspidella* is a member of the Menomoniidae and *Glaphyraspis* of the Lonchocephalidae. Holaspid morphologies of these two families are so different (for example, compare Pratt 1992, pl. 29, figs 20, 21 for *Bolaspidella* and pl. 26, figs 13, 14, 20 for *Glaphyraspis*) that the two families have not heretofore been considered as closely related to each other. Comparison of the larval morphologies of these two taxa with those of other Cambrian trilobites (Lee 2002) demonstrates that the protaspides of the two taxa share more similarities with each other than with those of any other Cambrian taxon. This suggests that the two taxa are closely related, and should be placed in the same higher taxon, most likely a new superfamily, yet to be erected. The shared larval characters would be synapomorphies of this taxon.

A recent classification of the Order Ptychopariida made by Fortey (*in* Whittington *et al.* 1997) incorporates about

Figure 12 SEM photographs of protaspides of species co-occurring with *Bolaspidella housensis* (Walcott, 1886). All pictures are × 100, unless otherwise noted. All specimens are from the Marjum Formation. (a, b, f, g) protaspis of Ptychopariide sp. A, UA 13504: (a) dorsal view; (b) ventral view; note that the librigenae and rostral plate are preserved intact; (f) posterior view; (g) anterior ventral view. (c, h, l) protaspis of Ptychopariide sp. A, UA 13505: (c) magnified view of hypostome, × 200; note the presence of nine hypostomal border spines; (h) dorsal view; (l) ventral view. (d, e) protaspis of Ptychopariide sp. A, UA 13506: (d) magnified view of hypostome, × 200; (e) ventral view. (i, m) protaspis of Ptychopariide sp. A, UA 13507: (i) dorsal view; (m) posterior view. (j) protaspis of Ptychopariide sp. A, UA 13508, dorsal view. (k) protaspis of Ptychopariide sp. A, UA 13509, dorsal view. (n, o, u) protaspid stage 1 of Ptychopariide sp. C, UA 13510: (n) magnified view of hypostome and rostral plate, × 200; note that posterior margin of rostral plate is transversely longer than anterior hypostomal margin; (o) ventral view; (u) dorsal view. (p, s, v) protaspid stage 2 of Ptychopariide sp. B, UA 13511: (p) magnified view of hypostome, × 200; (s) dorsal view; (v) ventral view. (q, r) protaspid stage 1 of Ptychopariide sp. B, UA 12830: (q) posterior view; (r) dorsal view. (t) protaspid stage 2 of Ptychopariide sp. C, UA 13512, dorsal view. (w, aa, bb) protaspis of Corynexochiide sp. A, UA 13513: (w) posterior view; (aa) dorsal view; (bb) lateral view. (x) protaspid stage 2 of Ptychopariide sp. B, UA 13514, dorsal view. (y) protaspis of Ptychopariide sp. D, UA 12825, dorsal view. (z) protaspis of Corynexochiide sp. A, UA 13515, dorsal view. (cc) protaspis of Ptychopariide sp. D, UA 13516, dorsal view.

https://doi.org/10.1017/S026359330000122X Published online by Cambridge University Press

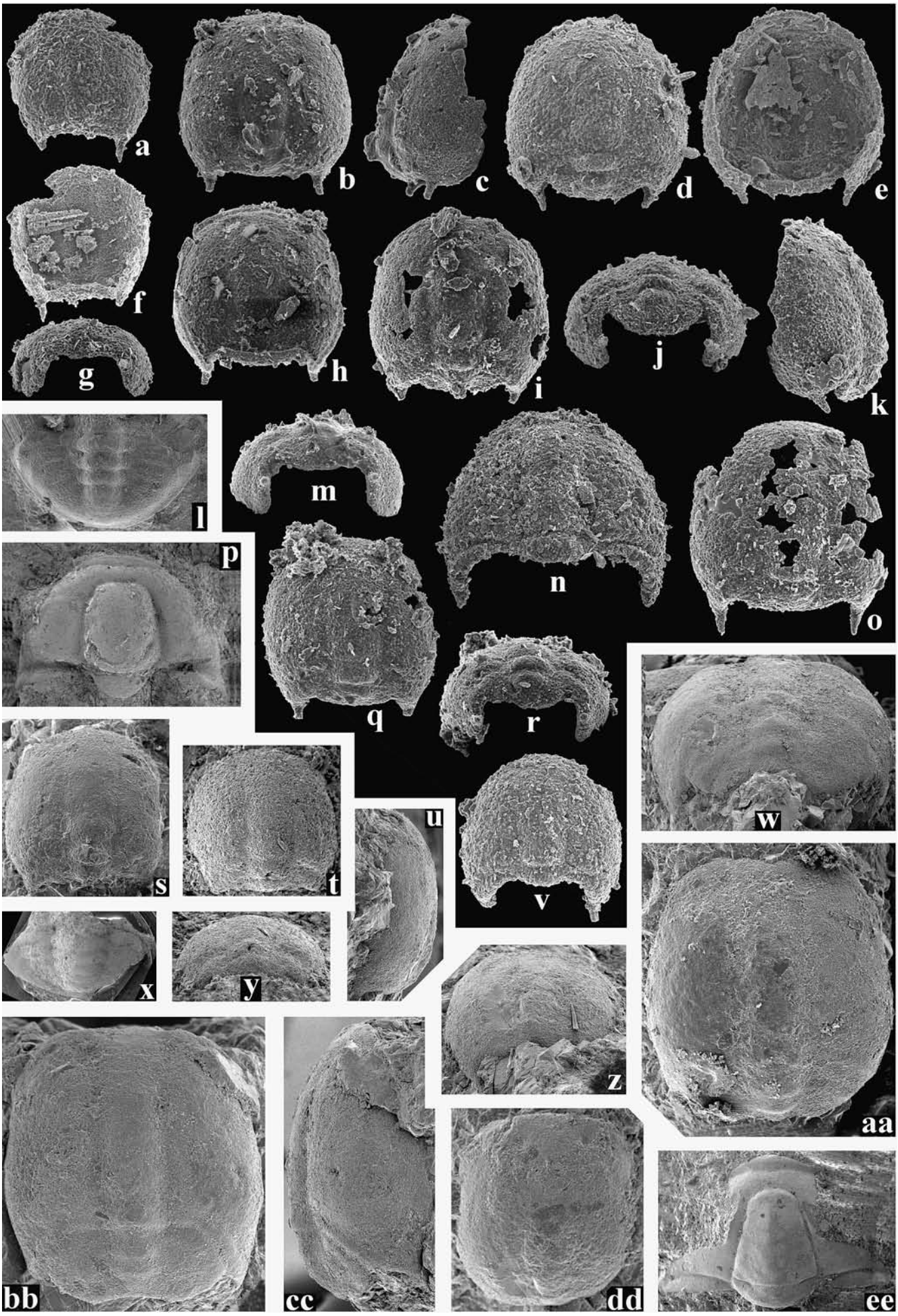

https://doi.org/10.1017/S026359330000122X Published online by Cambridge University Press

30 families assigned to the Superfamily Ptychoparioidea. Holaspid morphological information has failed to disclose relationships among these families, and biostratigraphic and palaeogeographic approaches have led to a superfluous number of unnatural (polyphyletic) groups. Morphological information provided by protaspides may help us to resolve this problem, if increasing morphological dissimilarity with growth can be recognised within the Ptychopariida and its phylogenetic implications are accepted.

An alternative explanation for the protaspid similarities is adaptation occurring in juvenile stages, decoupled from that occurring in adult stages. The similarities in the larvae could then be considered to be due in part to adaptation to ambient environments (for an example of trilobite workers, see Bergström 1977), and thus to be of little systematic value. However, such an *a priori* assumption of larval or adult homoplasies would discourage systematists from studying ontogeny and carrying out phylogenetic analysis where the goal is to find out monophyletic groups defined by homologous synapomorphies (Hennig 1966; Wiley *et al*. 1991). Rather than assuming homoplasies before an analysis, it is reasonable to reconstruct a phylogeny based on all available morphological data, including protaspid morphologies, and then read character distributions in the resultant phylogeny to assess whether each character is homologous or homoplasious.

5. Acknowledgements

The authors would like to thank the two anonymous reviewers for their constructive criticism. This project was supported by Korea Science and Engineering Foundation grant R01–2004–000–10167–0 to D-C Lee and grants from the Natural Sciences and Engineering Research Council of Canada to BDEC.

6. References

Beecher, C. E. 1895. The larval stages of trilobites. *The American Geologist* **16**, 166–97.

Bergström, J. 1977. Proetida – a disorderly order of trilobites. *Lethaia* **10**, 95–105.

Chatterton, B. D. E., Siveter, D. J., Edgecombe, G. D. & Hunt, A. S. 1990. Larvae and relationships of the Calymenina (Trilobita). *Journal of Paleontology* **2**, 255–77.

Edgecombe, G. D., Speyer, S. E. & Chatterton, B. D. E. 1988. Protaspid larvae and phylogenetics of encrinurid trilobites. *Journal of Paleontology* **62**, 779–99.

Hennig, W. 1966. *Phylogenetic Systematics*. Urbana and Chicago: University of Illinois Press.

Hu, C.-H. 1971. Ontogeny and sexual dimorphism of Lower Paleozoic Trilobita. *Palaeontographica Americana* **7**, no. 44.

Hu, C.-H. 1972. Ontogeny of three *Cedaria* Zone trilobites from Upper Cambrian, Montana. *Transactions and Proceedings of Palaeontological Society of Japan, New Series* **85**, 245–59.

Hu, C.-H. & Tan, L.-L. 1971 Ontogenies of two Upper Cambrian trilobites from Northern Black Hills, South Dakota. *Transactions and Proceedings of Palaeontological Society of Japan, New Series* **82**, 61–72.

Kobayashi, T. 1935. The Cambro-Ordovician formations and faunas of South Chosen. Palaeontology. Part 3. Cambrian faunas of South Chosen with a special study on the Cambrian trilobite genera and families. *Journal of the Faculty of Science, Imperial University of Tokyo, section II* **4**, 49–344.

Lee, D.-C. 2002. *Protaspides of Ptychopariida and taxonomy of Hystricuridae, with discussion of ancestry of Proetida*. Unpublished Ph.D dissertation, University of Alberta, Canada.

Lee, D.-C. & Chatterton, B. D. E. 2003 Protaspides of *Leiostegium* and their implications for membership of the order Corynexochida. *Palaeontology* **46**, 431–45.

Palmer, A. R. 1954. An appraisal of the Great Basin Middle Cambrian trilobites described before 1900. *United States Geological Survey, Professional Paper* **264-d**, 55–86.

Palmer, A. R. 1962. Comparative ontogeny of some opisthoparian, gonatoparian and proparian Upper Cambrian trilobites. *Journal of Paleontology* **36**, 87–96.

Pratt, B. R. 1992. Trilobites of the Marjuman and Steptoean stages (Upper Cambrian), Rabbitkettle Formation, southern Mackenzie Mountains, northwest Canada. *Palaeontographica Canadiana* **19**.

Resser, C. E. 1937. Third contribution to nomenclature of Cambrian trilobites. *Smithsonian Miscellaneous Collections* **95**, no. 22.

Robison, R. A. 1964. Late Middle Cambrian faunas from western Utah. *Journal of Paleontology* **38**, 79–92.

Robison, R. A. 1988. Trilobites of the Holm Dal Formation (late Middle Cambrian), central North Greenland. *Meddelelser om Grønland* **20**, 23–103.

Slack, J. M. W., Holland, P. W. H. & Graham, C. F. 1993. The zootype and the phylotypic stage. *Nature* **361**, 490–92.

Swinnerton, H. H. 1915. Suggestions for a revised classification of trilobites. *Geological Magazine* (*new series 2*) **6(2)**, 487–96; 538–45.

Walcott, C. D. 1886. Second contribution to the studies on the Cambrian faunas of North America. *United States Geological Survey Bulletin* **30**.

Walcott, C. D. 1899. Cambrian fossils of the Yellowstone National Park. *United States Geological Survey Monograph* **32**, 440–78.

Walcott, C. D. 1916. Cambrian geology and paleontology III, no. 3 – Cambrian trilobites. *Smithsonian Miscellaneous Collections* **64**, no. 3, 157–256.

Whittington, H. B., Chatterton, B. D. E., Speyer, S. E., Fortey, R. A., Owens, R. M., Chang, W. T., Dean, W. T., Jell, P. A., Laurie, J. R., Palmer, A. R., Repina, L. N., Rushton, A. W. A., Shergold, J. H., Clarkson, E. N. K., Wilmot, N. V. & Kelly, S. R. A. 1997. *Treatise on Invertebrate Paleontology, Part O, Arthropoda 1, Trilobita, Revised, Volume 1*. Boulder, Colorado and Lawrence, Kansas: Geological Society of America and University of Kansas Press.

Wiley, E. O., Siegel-Causey D., Brooks, D. R. & Funk, V. A. 1991. The Compleat Cladist: A Primer of Phylogenetic Procedures. *The University of Kansas and Museum of Natural History, Special Publication* **19**.

Figure 13 *Glaphyraspis parva* (Walcott, 1899), Ptychopariide sp. E, and *Apomodocia conica* Hu, 1971. All pictures are × 100, unless otherwise noted. Silicified specimens of *G. parva* (a–k, m–o, q, r, v) were recovered from the Dunderberg Formation and crack-out specimens (1, p, s, t, y) from the Deadwood Formation. Crack-out specimens of Ptychopariide sp. E (u, w, z-dd) and *A. conica* (x, ee) are from an unknown locality in northern Utah. (a, f, g) protaspid stage 1 of *Glaphyraspis parva*, UA 13517: (a) dorsal view; (f) ventral view; (g) posterior view. (b, c, h, m) protaspid stage 2 of *Glaphyraspis parva*, UA 13518: (b) dorsal view; (c) lateral view; (h) ventral view; (m) posterior view. (d, e, j, k) meraspid degree 0 of *Glaphyraspis parva*, UA 13519: (d) dorsal view; (e) ventral view; (j) posterior view; (k) lateral view. (i) protaspid stage 2 of *Glaphyraspis parva*, UA 13520, dorsal view. (l) holaspid pygidium of *Glaphyraspis parva*, CMC-P 40310c′, dorsal view, × 25. (n) meraspid cranidium of *Glaphyraspis parva*, UA 13521, dorsal view, × 75. (o) protaspid stage 2 of *Glaphyraspis parva*, UA 13522, dorsal view. (p) holaspid cranidium of *Glaphyraspis parva*, CMC-P 40310b′, dorsal view, × 18. (q, r) protaspid stage 2 of *Glaphyraspis parva*, UA 13523: (q) dorsal view; (r) posterior view. (s) protaspid stage 2 of *Glaphyraspis parva*, CMC-P 40310e, dorsal view. (t, y) protaspid stage 2 of *Glaphyraspis parva*, CMC-P 40310d: (t) dorsal view; (y) posterior view. (u, z, dd) protaspid stage 1 of Ptychopariide sp. E, CMC-P 38745c: (u) lateral view; (z) posterior view; (dd) dorsal view. (v) meraspid cranidium of *Glaphyraspis parva*, UA 13524, dorsal view, × 75. (w, aa) protaspid stage 2 of Ptychopariide sp. E, CMC-P 38725e: (w) posterior view; (aa) dorsal view. (x) holaspid pygidium of *Apomodocia conica*, CMC-P 38725p, dorsal view, × 6. (bb, cc) protaspid stage 2 of Ptychopariide sp. E, CMC-P 38725g: (bb) dorsal view; (cc) lateral view. (ee) holaspid cranidium of *Apomodocia conica*, CMC-P 38725, dorsal view, × 6.

https://doi.org/10.1017/S026359330000122X Published online by Cambridge University Press

DONG-CHAN LEE, Department of Museum, Daejeon Health Sciences College, 77-3, Gayang2-dong, Dong-Gu, Daejeon, 300–711 South Korea, and
Gyeryongsan Natural History Museum, 511-1 Hakbong-Ri, Banpo-Myeon, Gongju, Chungnam, 314–924 South Korea.

BRIAN D. E. CHATTERTON, Department of Earth & Atmospheric Sciences, University of Alberta, Edmonton, Alberta T6G 2E3, Canada.

MS received 26 April 2004. Accepted for publication 17 March 2005.